

Particle size and abundance measurements suggest temporally variable biotic transport and disaggregation in the Eastern Tropical North Pacific Oxygen Minimum Zone

Jacob A. Cram

07 January 2020

Author list

(Putative, order not set, Please suggest others.)

Jacob Cram, Clara Fuchsman, Megan Duffy, Jessica Pretty, Rachael Lekanoff, Jaqui Neibauer, Shirley Leung, Klaus Huebert, Thomas Weber, Danielle Bianchi, Allan Duvol, Rick Keil, Andrew McDonnel

Abstract

Models and observations suggest that particle flux attenuation is lower across the mesopelagic zone of anoxic environments compared to oxic ones. This attenuation is likely a function of microbial metabolism, as well as aggregation and disaggregation by zooplankton and other processes. The concentration of different sizes of particles in the ocean, called the particle spectrum, is shaped by particle aggregation, disaggregation and remineralization processes. Observing and modeling particle spectra can provide information about the contributions of these processes. We measured particle size spectrum profiles at one station in the oligotrophic Eastern Tropical North Pacific Oxygen Minimum Zone (ETNP OMZ) using an underwater vision profiler (UVP), a high resolution camera that counts and sizes particles. Measurements were taken at different times of day, over the course of a week. Comparing these data to particle flux measurements from sediment traps allowed us to constrain the particle size to flux relationship, and to generate highly resolved depth and time estimates of particle flux rates. We found that particle flux attenuated very little throughout the anoxic water column, and at some time-points appeared to increase. Comparison to the predictions models of particle dynamics in OMZs suggested slow remineralization of all sizes of particles, and disaggregation by zooplankton between the base of the photic zone and 500m. Acoustic measurements of multiple size classes of organisms suggested that many organisms migrated, during the day, to this region with high disaggregation. Our data suggest that migrating organisms both actively transport biomass and disaggregate particles in the OMZ core. Our data further suggest both within and between day variability in active transport and particle disaggregation.

Introduction

The biological pump, in which sinking particles transport carbon from the surface into the deep ocean, is a key part of the global carbon cycle (Neuer, Iversen, and Fischer 2014; Turner 2015). Organic matter flux into the deep ocean is a function both of export from the photic zone into the mesopelagic (export flux), and the fraction of that flux that crosses the mesopelagic (transfer efficiency) (Passow and Carlson 2012; Siegel et al. 2016; Francois et al. 2002). The transfer efficiency of the biological pump, may affect global atmospheric

carbon levels (Kwon, Primeau, and Sarmiento 2009). Thus understanding the processes that shape organic matter degradation in the mesopeleagic are critical.

Zooplankton play an important role in shaping carbon flux through the mesopeleagic (Steinberg and Landry 2017; Turner 2015; Jackson and Burd 2001), and by extension the efficiency of the biological pump (Cavan et al. 2017; Archibald, Siegel, and Doney 2019). They affect particle flux through *repackaging*, *respiration*, *active transport* and *disaggregation*. Zooplankton *repackage* particles into fecal pellets that have different properties from the original particles (Wilson, Steinberg, and Buesseler 2008). Zooplankton consume particles in the mesopeleagic and *respire* some of their biomass. It was found that this rate of consumption was less than flux in the California Current (Stukel et al. 2019). Zooplankton consume particles in surface depths and release it at others, thereby *actively transporting* carbon, usually downward (Archibald, Siegel, and Doney 2019; Bianchi et al. 2013; Hannides et al. 2009; Steinberg et al. 2000; Stukel et al. 2018, 2019). Zooplankton break large particles into smaller ones, likely by generating turbulence when they swim (Dilling and Alldredge 2000; Goldthwait et al. 2005). This *disaggregation* can lead to increased remineralization of particles because those smaller particle pieces sink more slowly and so have longer residence times, and so have longer to break down in the mesopeleagic (Goldthwait et al. 2005). In this manuscript we focus on active transport and disaggregation in particular.

Oxygen levels, and in particular anoxic regions of the water column, appear to modulate particle flux through the mesopeleagic. Observations of particle flux in the region of the Eastern Tropical North Pacific (Van Mooy, Keil, and Devol 2002; Hartnett 1998) that is near the Mexican coast, and Arabian Sea (Keil, Neibauer, and Devol 2016) have suggested lower flux attenuation in these OMZ systems. Models have shown that accounting for oxygen limitation in OMZs is necessary to fit global patterns of particle transfer (Cram et al. 2018; DeVries and Weber 2017). Oxygen minimum zones in the open ocean are expanding (Stramma et al. 2008), and this expansion is likely to effect ocean chemistry, the habitat of marine organisms, and the interactions between between organisms and chemistry (Gilly et al. 2013). Models and chemical data suggest that oxygen minimum zones may enhance carbon transport to the deep ocean, by inhibiting microbial degradation of sinking marine particles (Cram et al. 2018). However, biological organic mater transport is modulated by zooplankton (Steinberg et al. 2008; Steinberg and Landry 2017) which feed on, produce and disaggregate particles, and whose interactions on particle flux in pelagic OMZs are only beginning to be explored (Kiko et al. 2020).

Models of particle transfer through the mesopeleagic oceans suggest that particle size, ocean temperature, and oxygen concentrations modulate particle flux (Cram et al. 2018; DeVries and Weber 2017). Meanwhile regional differences in particle ballasting play a smaller role. (Cram et al. 2018). These models, however, assume that zooplankton play a small role, and therefore assume no transport through the mesopeleagic, and no disaggregation. As a result of this assumption, the models predict that small particles will attenuate with depth. However small particles have been shown to persist in deep waters (REF) and contribute substantially to flux in the deep ocean (REF {I've seen this somewhere but am having trouble finding the reference}). Conveniently, these models' particle size predictions generate a useful null hypothesis of expected particle size distributions in the absence of zooplankton effects. Thus their predictions can, in principle, be compared to observed distributions of particles to explore the magnitude of zooplankton effects.

Underwater vision profilers, cameras that can count and size many particles over large water volumes (Picheral et al. 2010), provide valuable information about particle transport. When deployed in concert with particle traps in some regions, they can be used to predict flux in other regions where traps have not been deployed (Guidi et al. 2008; Kiko et al. 2020). UVP can furthermore provide resolved information about particle flux variability across space and time (Guidi et al. 2008; Kiko et al. 2017). Connecting UVP and trap data can furthermore inform about relationships between particle size, biomass, and sinking speed, as well as the contributions of the different particle sizes to flux (Guidi et al. 2008).

A recent study combined particle size tracking, mockness tows, and acoustic data, collected at one site, with trap measurements from nearby locations, from in literature, to explore zooplankton transport in the Eastern Tropical North Atlantic, a weak (hypoxic rather than fully anoxic) OMZ (Kiko et al. 2020). The authors found a particle maximum in the mesopeleagic and contended that this feature suggests transport by zooplankton, and mortality of migrating zooplankton. The authors suggest that in more anoxic and larger

OMZs, such as the modern day ETNP, and in particular or OMZs in the future, there might be less active transport into the mesopelegic than seen at their site, since migratory organisms would presumably not migrate as deeply into the water and would be less active in true OMZs. In this manuscript we provide data from such a truly hypoxic region.

A recent modeling study poses three hypotheses, each with a prediction about particle size distributions (Weber and Bianchi 2020). These are: **HWB1:** All particles in OMZs remineralize more slowly than in oxic water, regardless of their size. **HWB2:** There is less disaggregation by zooplankton in OMZs than elsewhere. **HWB3:** Large particles remineralize more slowly in OMZs, but smaller ones do not. This last hypothesis was indicated by model results that suggest that large particles are diffusion limited. Therefore, microbial metabolism in their cores could also be limited by Nitrate and Nitrite, even though both elements are present in the OMZ core. In that case less efficient sulfur oxidation processes would dominate (Bianchi et al. 2018). The authors propose that the processes underlying each hypothesis would have signature effects on particle size distribution in the core of the ETNP. The model with slow attenuation of all particles, predicts an increase in the abundance of small particles, while the other two models, predict a decrease in small particle abundance, because small particles are either not replaced by disaggregation of large particles (Model 2) or because those particles are remineralized more quickly than larger particles (Model 3). However, the authors were not able to support any hypothesis at the exclusion of the others because they did not have the necessary data about particle size. In this manuscript we present data that can test these three hypotheses.

Additionally, combined measurements of particle numbers, flux and migration of plankton, while available in the hypoxic ETNA (Kiko et al. 2020), have not been made in a fully anoxic region. Indeed the ETNA study used trap data from earlier studies. Thus while UVP and traps have been sampled together (Guidi et al. 2008), combined trap and UVP measurements have not been taken together previously in an OMZ. Globally, most of the volume of OMZs below regions of very low surface productivity (Fuchsman et al. 2019; Pennington et al. 2006). Meanwhile most flux data has been measured in higher productivity regions of the ETNP (Van Mooy, Keil, and Devol 2002; Hartnett 1998). Furthermore, the degree to which zooplankton swimming or other processes lead to particle disaggregation, both in OMZs and elsewhere in the ocean, is unknown.

To provide the data to test hypotheses and illuminate zooplankton particle interactions in oligotrophic OMZs, we collected particle size data at high temporal resolution over the course of a week in an anoxic site typical of the oligotrophic ETNP OMZ, well away from the high productivity zone in the coast. We integrated this size data with observed flux measurements, and acoustic data. We quantified, throughout the water column, how changes in size distribution deviate from changes that would be predicted by remineralization and sinking only models.

We ask the following three questions: **A:** How do the particle size distribution at one location in the oligotrophic Eastern Tropical North Pacific vary with respect to depth and time? **B:** Do our data support any of the three Weber and Bianchi (2020) models? **C:** Do our data suggest regions of the oxygen minimum zone with disaggregation like processes, and if so, do these co-occur with regions suggested to harbor zooplankton.

We hypothesized **H1:** Temporal day to day variability in particle number, particle size distribution slope and flux would be evident. **H2:** This variability would relate to the location of migratory zooplankton, with a combination of increased particle flux and disaggregation present where zooplankton occur. **H3:** Disaggregation and particle production by zooplankton might lead to particle size patterns that cannot be explained by remineralization and sinking alone. We also will test each of the three Weber-Bianchi models, specifically that OMZs have (**HWB1**) slower attenuation of all particles, (**HWB2**) decreased disaggregation, or (**HWB3**) slower attenuation of just large particles, in the OMZ core.

Methods

Unless specified otherwise, measurements were taken on board the R/V Sikuliaq from 07 January 2017 through 13 January 2017 at 16.5°N 106.9°W, located in an oligotrophic region of the Eastern Tropical North Pacific Oxygen Minimum Zone (ETNP Station P2; Figure 1A). Data are compared against measurements

taken at 16.5°N 152.0°W on 08 May. A same latitude region west of the OMZ, where oxygen is not limiting (P16 Transect Station 100; Figure S1).

Water property measurement

We measured water properties of temperature, salinity, fluorescence, oxygen concentration and turbidity using the shipboard XXX CTD {get sensor information}. Data were processed using Seabird Software and analyzed and visualized in *R*.

Particle size measurements

Particle size data were collected by Underwater Vision Profiler 5 (UVP) that was mounted below the CTD-rosette and deployed for all CTD casts shallower than 2500 m. A UVP is a combination camera and light source that describes the abundance and size of particles from $100\mu\text{m}$ to several centimeters in size (Picheral et al. 2010). Particles have been previously shown to be primarily “marine snow” but may also include a small number of zooplankton and visual artifacts. UVP data were processed using custom MATLAB scripts, uploaded to EcoTaxa (Picheral, Colin, and Irisson, n.d.), and analyzed in R. The UVP provided estimates of particle abundances of particles in different size-bins, as well as information about the volumes over which those particle numbers had been collected.

Flux measurements

Particles were collected in incubating particle traps ({Someone in Ricks’ lab – what is a good reference for these?}). Traps were used to perform incubation studies which will be reported elsewhere. As part of these studies, the traps also generated data about carbon flux, which is reported here. Two types of traps were deployed. We utilized two kinds of traps. One set of traps, generally deployed in shallower water, had a solid cone opening with area 0.46m^2 . The second set had larger conical net with opening of 1.23m^2 area made of $200\mu\text{m}$ nylon mesh. In all cases, particles collected in the net or cone fell into one of two chambers. The “plus-particles” chamber collected particles from the net and incubated them for approximately 22 hours. The top-collector trap collected particles, and then returned immediately to the surface. We preferentially used data from the “top-collector”. However in many cases, due to trap malfunctions, data was only available from the “plus-particles” trap, in which case we used that data.

Analysis

All analyses were constrained to the mesopelegic, defined here as the region between the base of the photic zone (175 m), which is below the oxycline, and 1000 m. For many analyses particles were binned by depth with 20 m resolution between the surface and 100 m, 25 m resolution between 100m and 200 m depths and 50m resolution between 200m and 1000m. To perform this binning, particle numbers, and volumes of water sampled of all observations within each depth bin were summed prior to other analyses.

Two normalized values of particle numbers were calculated. In the first, particle numbers were divided by volume sampled, to generate values in $\text{particles}/\text{m}^3$. In the second, particles were divided by both volume sampled and the width of the particle size-bins to generate values in $\text{particles}/\text{m}^3/\text{mm}$.

Particle size distribution

We determined the slope and intercept of the particle size distribution spectrum by fitting a power law to the data. Because large particles were infrequently detected we used a negative-binomial general linear model that considered the volume of particles sampled, and particle bin-size and that assumed that the

residuals of the data followed a negative-binomial (rather than normal) distribution. Thus we fit the equation $\ln\left(\frac{E(\text{Total Particles})}{\text{Volume} * \text{Binsize}}\right) = b_0 + b_1 \ln(\text{Size})$ to solve for the Intercept (b_0) and particle size distribution slope ($PSD = b_1$). Where the term on the left describes the expected volume and bin-size normalized count data, assuming a negative binomial distribution of residuals.

Estimating particle flux

We estimated particle flux throughout the water column, by fitting particle data to trap measurements. We assumed that particle flux in each size bin (j) followed the equation

$$\text{flux}_j = \left(\frac{\text{Total Particles}_j}{\text{Volume} * \text{Binsize}_i} \right) * C_f * (\text{Size})^a$$

(Eqn 1.)

And where flux at a given depth is the sum of all bin specific values.

$$\text{Flux} = \sum_j \text{flux}_j$$

(Eqn 2.)

We used the `optimize()` function *R*'s `stats` package to find the values of C_f and a that yielded closest fits of the UVP estimated flux to each particle trap.

We also estimated the exponent of the particle size to biomass exponent α and size to sinking speed exponent γ per the equations $Biomass_j \sim \text{Size}_j^\alpha$ and $Speed_j \sim \text{Size}_j^\gamma$. This is done by assuming a spherical drag profile, in which case $a = /alpha + /gamma$ and $\gamma = \alpha - 1$ (Guidi et al. 2008).

Size specific information

We separately analyzed total particle numbers, particle size distribution, and particle flux for particles larger than or equal to $500\mu\text{m}$, and those smaller than $500\mu\text{m}$, to determine the relative contributions of these two particle classes to particle properties.

Variability

We used a general additive model, of form $Flux \sim s(\text{Depth}) + s(\text{Day}) + s(\text{Hour})$ to explore whether estimated flux levels appeared to vary by day and hour, holding the effects of depth constant, in the 250 m to 500 m region. The smooth terms s for “Depth” and “Day” were thin plate splines, while the s term for “Hour” was a cyclic spline of 24 hour period.

Modeling remineralization and sinking

We modified the Particle Remineralization and Sinking (PRISM) model, as described by DeVries et al. (2014) to estimate particle size distributions at each depth in the water column from (1) the particle size distribution in the depth bin above, and (2) the estimated change in flux between the two depths (which is itself calculated from the two observed distributions) (Supplement). The model generates a predicted profile at the deeper depth, which can be compared to the shallower depth.

Results

Physical and Chemical Data

The anoxic zone, characterized by undetectable oxygen levels, extends from 80 m to 850 m depth, with a sharp upper oxycline and a gradual lower oxycline (Figure 1B-D). The upper oxycline tracks a sharp pycnocline (Figure 1C-1D), characterized by a abrupt drop in temperature below the mixed layer, and an increase in salinity (Figure 1B). The site is characterized two fluorescence maxima (Figure 1C). The larger, shallower fluorescence peak is positioned just above the oxycline, ending exactly where oxygen reaches zero. The smaller, lower peak is positioned entirely inside of the anoxic zone. Turbidity tracks the two chlorophyll peaks in the surface, and has a tertiary maximum at the lower oxycline (Figure 1D).

Acoustic data reveal diel migration patterns

Acoustic data, produced by the shipboard EK60 , suggest the presence of multiple cohorts of migratory organisms. We focus initially on backscattering measurements from the EK60's lowest frequency 18000 Hz signal, because it travels furthest into the water column and has the best resolution of the channels. Most migratory organisms appeared to leave the surface at dawn and return at dusk, spending the day between 250 and 500m (Figure 2A). There appeared to be two local maxima in backscattering intensity at mid-day, one at ~300m and one at ~375 m (Figure 2A). There also appeared to be organisms that migrated downward at dusk and upward at dawn , spending the night at ~300m (Figure 2B). There was also a peak of organisms that appeared, at mid-day, on some but not all days, without any visible dawn or dusk migration just above the base of the photic zone. (Figure 2C). Some diel migrants appeared to cross the OMZ and spend the day below the detection range of the EK60 (Figure 2D), as well as organisms that appeared between 500m and 1000m but did not appear to migrate to or from that depth at our site, but rather traveled through the the EK60's field of view (Figure 2D).

Similar patterns were evident each other measured frequency, with better resolution by the lower frequencies (Figure S2).

Flux data from traps

Flux measurements at station P2 were consistent between the different particle trap types and chambers, and showed a profile that broadly followed a power law with respect to depth, with the exception that flux appeared to increase in one trap at 500m. Four traps in the surface had anomalously low measurements of flux, compared to similar traps placed at similar depths, which may have been due to trap malfunctions (Figure 3).

Particle abundance measurements vary with size and depth

In all profiles, particle abundances were highest at the surface, and highest among the smallest particles (Figure S3). Visual examination of the relationship between particle number and size suggested a power law relationship where the log of volume and bin-sized normalized particle abundance was proportional to the log of the particles' size (Figure S4). The exception to this pattern was very large particles, which are rare enough that they are usually not detected by the UVP. Generalized linear models that assume a negative-binomial distribution of the data were able to account for this under-sampling of large particles to estimate power law slopes, while considering rare occurrences of the large particles at each depth (Figure S4).

Total particle numbers were generally similar between different casts, regardless of which day or hour they were collected (Figure S5A). Particle numbers were highest in the surface and decreased rapidly, flattened out over the 250 m to 500m range, decreased again until the lower oxycline, and then increased below the oxycline (Figure S5A).

The particle size distribution slope steepened (became more negative) between the surface and 500m, flattened (became less negative) between 500m and 1000m, and then steepened again after 1000m (Figure S5B). Steeper, more negative, slopes indicate a higher proportion of small particles relative to large particles, while flatter, less negative, slopes indicate a higher proportion of large particles.

Estimated particle flux sometimes increases with depth in the OMZ core

Our optimization approach suggested that there was greatest agreement between estimates of trap observed particle flux, and UVP estimated particle flux when the particle size to flux relationship was governed by the ratio $Flux = 133 * Size^{2.00}$. Applying this fit to the UVP data resulted in a UVP predicted flux profile that broadly fit the expected trap observed flux profiles. This fit excludes the four traps that were held out from the analysis due to low abundance.

Particle flux profiles varied notably between casts between the base the photic zone and 500m m (Figure 4A-4B). Between 250 m and 500 m particle flux appeared to increase on some, but not all, casts, while attenuating slowly on the other casts (Figure 4C). Below 500m, there were not enough casts to measure variability between casts.

General additive models that examined the rate of change of flux between 250 and 500m found that, after removing the effect of depth, there was a statistically significant relationship between day of the week and the fifth-root transformed, rate of change of flux ($p = 0.002$), as well as between hour of the day and flux ($p = 0.040$) (Figure S6). There were increases in flux over this region towards the beginning and end of the sampling period, and lowest near day 10. There was also increases in flux in the daytime relative to night-time. By comparing three general additive models, one that considered only depth, one that considered depth and day of the week, and one that considered depth, day of week, and time of day, we found that depth accounted for 37% of the variance, adding day of the week accounted for an additional 18% of the variance, and hour of the day accounted for 8.7% of the remaining variance in transformed rate of change of flux. If the fifth root transformation was not applied to the rate of change of flux, the hourly pattern was not evident. Increases in flux in this region were clearly not limited to the daytime, as one midnight cast showed increases here as well (Figure 4C).

ETNP particle dynamics differ from those seen at an oxic site

The oxic site, P16 Station 100, was characterized by a more gradually sloping pycnocline, and an oxygen minimum at 500m of $19.7 \mu M$, which is not anoxic (Figure S1B). The photic zone is characterized by a single fluorescence peak with a maximum at 110m and which disappeared at 200m (Figure S1C). Turbidity followed chlorophyll concentration and did not have a peak in the mesopelegic (Figure S1D), unlike the ETNP site. There was a salinity peak at 150m (Figure S1B).

Particle numbers were higher, between the base of the photic zone through 1000m at the ETNP site, than at the same-latitude, oxygenic P16 station 100 (Figure S7A). Particle size distributions were similar between the two sites above 500m, being characterized by overlapping confidence intervals generated by a general additive model. From 500 to 1000m, particle size distributions were steeper at the ETNP site, being characterized by a higher proportion of small particles (Figure S7B).

Small particles ($100 \mu m - 500 \mu m$) at the ETNP site were about two orders of magnitude more common than large particles ($>= 500 \mu m$) (Figure S8). Large particle numbers appeared to attenuate more quickly than small particles, and more generally follow a power law decrease, while small particles appeared to increase around 500 m. Flux was predicted to be predominantly from small, rather than large particles, at all depths except the very surface. The particle size distribution, calculated only on large particles, was more variable between depths than calculated for small particles. Data from the oxic P16 station 100 suggested more particles, steeper particle size distribution, and more flux than at this station than at the ETNP station. They also suggested that differences between large and small particles, with respect to number, flux and size distribution that were broadly similar to the ones seen at ETNP Station P2.

In contrast to the anoxic station, at the oxic station, flux always decreased with depth (Figure S9A+B).

Smoothed and averaged data

Highly smoothed particle data suggested that particle size, averaged across all casts, followed a pattern in which the abundance of small particles increased in the OMZ surface (Figure 5A), which corresponded with steepening of the particle size distribution (Figure 5A), an increase in small particle biomass (Figure 5B), but not of large particle biomass (Figure 5C). Deeper in the OMZ, the small particle number, PSD slope, and biomass of small particles declined. At the oxic site, particle size distributions generally steepened with depth, while both small and large particle estimated biomass followed a power law decrease with depth.

Particle number dynamics differ from model expectations

We were able to use our modified particle remineralization and sinking model to predict particle size distributions at each depth from the particle size distribution one depth-bin shallower and the calculated flux attenuation between the two depths. We found that the observed particle size distributions usually varied from model expectations (Figure S10). Tautologically, at each depth, the observed size profile and the model predicted size profiles have same flux. However, the difference between the flux of observed and predicted *small particles* ($100 - 500\mu\text{m}$), normalized to depth, serves as a metric of patterns of deviations from modeled results. We call this value *OSMS* (Observed Small Flux Minus Modeled Small Flux).

$$\text{OSMS} = \frac{(\text{Small Flux Observed} - \text{Small Flux Modeled})}{\Delta Z}$$

Eqn. 3

In the above equation ΔZ is the distance, in meters, between the current depth bin and the previous depth bin, whose particle size distribution is fed into the predictive model.

OSMS was positive between the photic zone and 500 m, meaning that less small flux attenuated than would be expected from the *PRISM* model in this region. There was some variability in the OSMS parameter between casts. A general additive model, after factoring out the effect of depth, found that there was a statistically significant relationship between day of the cast and OSMS with highest values near day 10 of the study (which is when flux attenuation in this region was lowest) ($p=0.01$) (Figure S11). However there was not a statistically significant relationship between hour of the day and OSMS.

Below 500 m, OSMS was negative. There were only two casts that reached below 500m at this station, and so an analysis of the dynamics of OSMS in this region are not possible.

At P16 Station 100, OSMS was positive between the base of the photic zone and 350m and negative below 350m (Figure S9C).

Discussion

Diel migrators spend time in the OMZ core

Organisms of all sizes appear to migrate into the core of the OMZ at our site. Most migrators appear to leave the surface at dusk, spend the day in the top 500m of the OMZ in the day and return to the surface at dusk (Figure 2A), while others show the opposite pattern, leaving the surface at dusk and returning at dawn (Figure 2B). Diel migration is prevalent throughout the oceans (Hays 2003; Cisewski et al. 2010; Heywood 1996; Jiang et al. 2007; Rabindranath et al. 2011; Yang et al. 2019; Sainmont et al. 2014), including other OMZ sites (Antezana 2009; Kiko et al. 2020; Riquelme-Bugueño et al. 2020), including highly anoxic sites

with secondary, anoxic deep chlorophyl maxima like this one (Hidalgo, Escribano, and Morales 2005), and much of the ETNP OMZ (Herrera et al. 2019). Sampling efforts elsewhere in the ETNP suggested that any of these diel migrants are euphausiids and fish (Maas et al. 2014; Wishner et al. 2013), and that diel migrants are primarily 2-5 mm in size (Wishner et al. 2013). Krill in the Humboldt current OMZ, migrate to the surface at night (Riquelme-Bugueño et al. 2020), as seen for some organisms at our site (Figure 1B). The presence of organisms that appear and disappear just above the base of the photic zone, in the region of the deeper anoxic fluorescence peak region, but absence of a tell-tale signature of mass migration before or after they appear (Figure 1C) may suggest that these organisms migrate at different times of the day to this deep region, rather than all at once. Another possibility is that they are transiting through our station at this depth in mid day, but do not migrate to depth at this location, but rather at another location.

The organisms that appear between 500m and 1000 m (Figure 2E) have acoustic signatures that resemble jellyfish (Kaartvedt et al. 2007). That they appear in horizontal bands that do not appear to trend upwards over time suggests that they are traveling through our site at progressively shallower depths over the course of the day, but that individual swarms are not themselves moving upward at this station. This suggests that any vertical migration carried out by these organisms happens elsewhere, or occurs more slowly than the advection seen at this site. That they appear at different depths at different times of the day suggest that these organisms have some sort of vertical migration pattern. Future work may consider more highly resolved spatial and temporal monitoring of this phenomenon. Indeed molecular surveys have found evidence of both Cnidarians and Ctenophores both within and below the ETSP OMZ near Chile (Parris et al 2014).

Flux is lower at this site than previous measurements in the ETNP

Flux at our site is lower at all depths than seen in previous measurements by traps at other, more productive, OMZ sites (Van Mooy, Keil, and Devol 2002; Hartnett 1998).

The flux to size relationship is typical of other sites.

The exponent of the particle size to flux relationship that we saw at our site 2.00, is of a similar magnitude to those seen by other studies that compare UVP flux to trap flux (Guidi et al. 2008; Kiko et al. 2020). It is slightly smaller than those measurements. This could be because these values vary between sites, or that imprecision in flux measurements leads to differences in these values between studies. Indeed, we found this value was sensitive to outlying data points.

In our analysis, we removed four traps that measured very little flux in the surface from our fitting algorithm. If we left these traps in our analysis, we instead got values for this size relationship exponent that approached zero. Because we have found that traps appear to under-measure flux when they fail, rather than over measure it, we have gone with the higher measurements.

Remineralization rates of all particles decrease in the OMZ, but disaggregation does not

Particle size profiles, particle size distribution slopes, and estimated biovolume, averaged across all casts and smoothed, are all similar to the predictions made by Weber and Bianchi's (2020) "Model 1". (Figure 4), and therefore our hypothesis **HWB1**. This suggests that the low oxygen at this site decreases the particle remineralization rate of all particles, including small ones. It does not support the Weber-Bianchi Model 2 in which remineralization is suppressed in the OMZ, nor their Model 3 in which only the very large particles' remineralization is slowed. The data at the oxic site, generally conformed to Weber and Bianchi's "Model 0" (2020), which was their prediction for particle distributions at oxic sites. However, one difference was that the observed particle size distribution, while essentially constant from the base of the photic zone through 1000m, appeared to steepen between 1000 and 2000m, suggesting an increase in the abundance of small particles,

relative to Model 0. This could indicate increased disaggregation in this region or horizontal transport of small particles through advection in this region.

Zooplankton likely transport organic mater into the OMZ core.

Predicted flux levels sometimes increase between 275 and 625 meters, and at all other times attenuate very slowly in this region. The EK60 data suggest the diel migration of all sizes of organisms to this region. Taken together, the concurrent increase in flux concurs and diel migration, suggest transport of organic mater by zooplankton. That the flux varies between days suggests some day to day variability in this transport. That flux is highest in the day, on average, suggests that the diel migrators may be contributing to this flux, but the fact that this diel variability is small compared to overall variability suggests that additional factors may modulate active transport, and that nocturnal migrators may also play a role in carbon transport.

Zooplankton likely disaggregate particles in the OMZ core.

The observation that there is greater flux by small particles ($< 500 \mu\text{m}$) than would be predicted by remineralization and sinking alone (Figure 9), between the photic zone and 500 m suggests that some process is disaggregating large particles into smaller ones. That this corresponds with the region where migratory organisms are found suggests that some of these organisms, likely small animals such as copepods and euphausiids (Herrera et al. 2019; Maas et al. 2014), may break down particles (Goldthwait et al. 2005; Dilling and Alldredge 2000). Alternatively, other processes such as horizontal advection of water containing small particles (Inthorn 2005) could be responsible for this increase in small particles .

Other deviations from model assumptions could also explain the increase in small particles relative to model predictions. For instance, if the model's assumed relationships between size, flux, sinking speed and biomass are not all accurate, particle dynamics would also differ. For instance, if remineralization differed between particle types, with small particles breaking down more slowly than larger ones, we might see the same kind of deviation from the model. If small particles sank more quickly for their size than expected, as has been seen elsewhere (McDonnell and Buesseler 2010), a similar deviation would occur as they would have less time to remineralize per depth.

Our model also assumes a spherical particle drag profile, such that the particle sinking speed fractal dimension (γ) is one less than the particle size fractal dimension (α) (Cram et al. 2018; Guidi et al. 2008), and that these two values sum to the particle flux fractal dimension. If any of these assumptions do not hold, or if our calculation of the particle flux fractal dimension was in error, the magnitude of the values may differ.

Furthermore, since flux varies over time, that variability could contribute to our observed patterns. We have not deconvolved temporal variability from model effects these processes, but future models could leverage time series data like this one to incorporate multiple observed time-points into the prediction of particle size distributions at depth. One way to do this would be to use a smoothing function to interpolate particle abundances at each size, depth and times, and then to use a model in which the sinking speed of a given particle size is used to identify the relevant time-point where the abundance informs that time-point.

In contrast to the upper OMZ core, there is an apparent flattening of the particle size distribution below 500 m, beyond the expected effects generated by particle remineralization. This could suggest aggregation processes (Burd and Jackson 2009). Indeed, aggregation could be occurring throughout the OMZ core, but only exceed disaggregation in this region.

Revisiting Hypotheses

Our data provide the first combined look at the relationship between particle size, particle flux and migratory organisms. Our data support only the first of the Weber-Bianchi hypotheses (Weber and Bianchi 2020), that particles of all sizes remineralize more slowly in OMZs **HWB1**. It did not support Weber and Bianchi's

hypotheses that disaggregation is lower in the OMZ **HWB2**, nor that the largest particles degraded particularly slowly in OMZs **HWB3**. This non-support of the final hypotheses, that large particles do not degrade particularly slowly surprised the authors, since models suggest that remineralization in the largest particles is driven by sulfate reduction, which is not as efficient as other processes (Weber and Bianchi 2020).

While we hypothesized temporal within and between day variability in particle size, number and flux **H1**, we only observed statistically significant temporal variability in flux, and this variability was relatively small, compared to the total amount of flux. Flux was, in general, highest in the day-time, suggesting transport by diel migrators, but this variability was not very strong. This suggests, that particle sinking speed may be slow enough that the diel migratory patterns of zooplankton occur on a shorter time-scale than that at which particles sink out of different water column layers. Careful analysis of particle sinking speed estimates would help to zero in on these time scales, but is beyond the scope of the current manuscript. That the decreased flux attenuation happened more in the day, and primarily in the DVM region supported our **H2** that changes in flux corresponded with migrator abundances.

Our data supported our hypothesis particle size patterns cannot be explained by remineralization and sinking alone **H3**. Indeed the abundance of small particles above 500m, suggested either the presence of disaggregation, or another process.

Opportunities for future directions

Our model can produce particle remineralization rate estimates and show how this rate changes throughout the water column. We did not include those estimates in this manuscript, because those estimates appear to be influenced by active transport into the Diel Vertical Migration (DVM) region. However, with corrections, or by focusing on the OMZ region below the DVM, it may be possible to estimate particle remineralization rates in OMZs from UVP measurements, and possibly compare these to variations in temperature and oxygen concentration, which we have previously suggested to influence particle remineralization rates (Cram et al. 2018).

We have only done these calculations at one station. We focused on one station in order to quantify within and between day variability, and found this variability to be present, but low. Thus, it is now possible, if more OMZ measurements were to be collected by UVP elsewhere in the ETNP or other OMZ regions, to use our model to determine Weber and Bianchi's (Weber and Bianchi 2020) Model 1, that particles of all sizes break down more slowly in OMZs, applies elsewhere.

Similarly, a clear next step is to apply our disaggregation model to other ocean regions. Indeed data are already collected by other groups (Guidi et al. 2008; Kiko et al. 2017, 2020). Temporal variability only has a smallish role in stuff, it may be reasonable to explore disaggregation like processes without the time-series in other environments, such as globally.

Conclusions

Particles of all sizes appear to remineralize more slowly at this OMZ site than in oxic sites. Furthermore, it appears that diel migratory organisms both disaggregate particles and transport carbon throughout the top 500m of the water column. Day to day and within day variability in organic matter transport was evident, though overall patterns in particle size, flux and disaggregation appeared to be consistent over the course of the time-series.

Figures

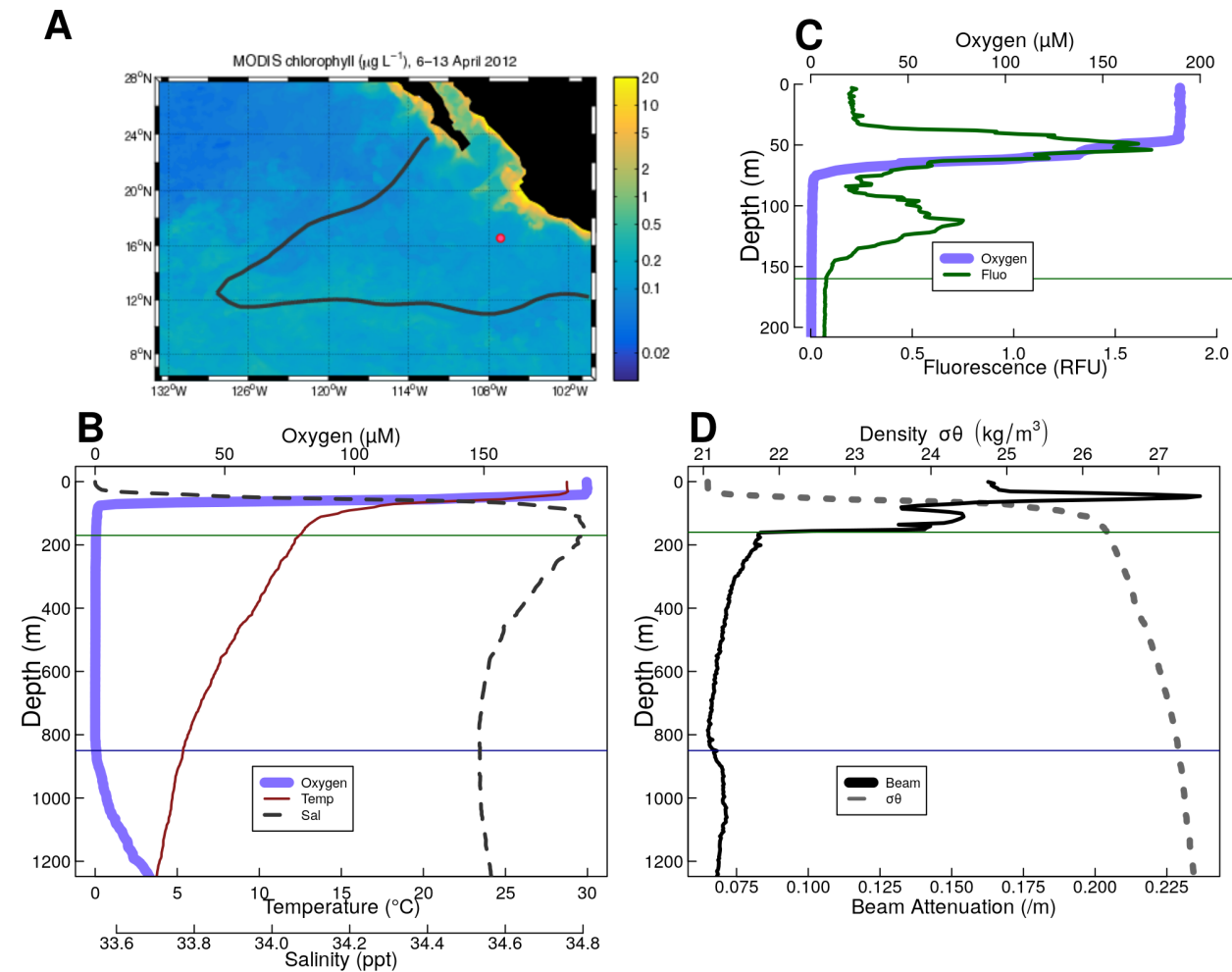


Figure 1. Overview of the geography, physics and chemistry of ETNP station P2 (A) Map of the ETNP Oxygen Minimum Zone and the location of station P2. Colors indicate chlorophyll concentrations at the surface, while the red outline signifies the region containing low oxygen. The red circle indicates the location of Station P2. (B-D) Oceanographic parameters collected from a cast at 2017-01-13 12:15 CST (local time). All profiles contain a plot of oxygen concentrations. When available, the thin horizontal green line shows the location of the base of the photic zone (160m), while the horizontal blue line shows the base of the oxycline. Figures B and D also show density (Dashed Gray Line). (B) highlights temperature and salinity. (C) fluorescence, focusing on the top 300m of the water column, and (D) beam attenuation.

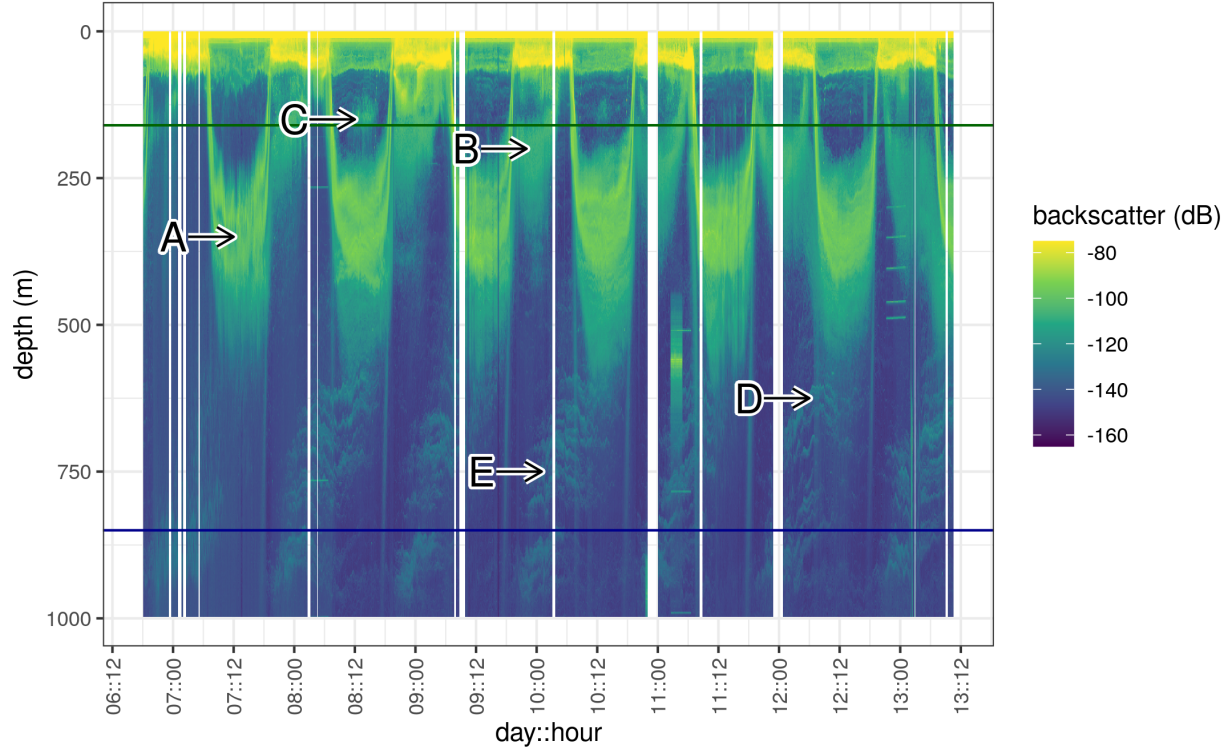


Figure 2. Acoustic data, measured by EK60, measured over the course of the experiment. Shown are data from the 18000 Hz frequency band, which have highest depth penetration, but which appear to co-occur with data from other frequency bands (see Figure SX). Values are in return signal intensity and have not been normalized to observed biomass. Several interesting patterns can be seen. **A.** Two bands of organisms can be seen leaving the surface at dawn, spending the day between 250 and 500m and returning to the surface at dusk. **B.** Another group of nocturnally migrating organisms can be seen leaving the surface at dusk, spending the night near 250m and returning at dawn. **C.** Some organisms appear at the base of the photic zone, during some, but not all mid days, and then disappear in the evening. **D.** A group of very deep migrating organisms appears to leave the surface with the diel migrants and pass all the way through the OMZ and out of the EK60's field of view. It returns at dusk. **E.** Swarms of organisms appear between 500 and 1000m disappearing later in the day. Swarms appear in the deepest layers at night and appear progressively shallower as the day progresses.

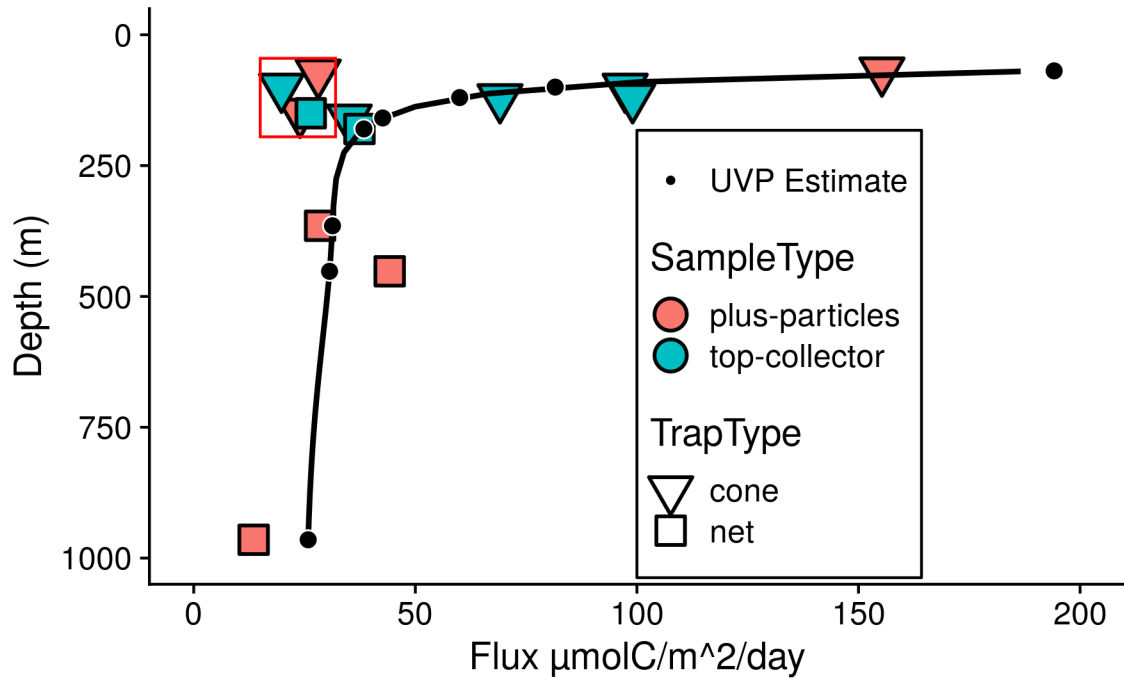


Figure 3. Particle flux, measured from sinking traps large symbols. Data from the “plus particles” and “top collector” samples from both cone and net traps were collated to generate these data. Trap types are shown by the shape and color of the large points. Superimposed are binned estimates of particle flux generated by fitting the sum of particle numbers all four profiles, binned as in Figure X, to the trap observed flux. The four points enclosed by the rectangle are unusually low compared to other traps collected at the same depth, and were therefore excluded from the fit. {Convert UVP points to a line, maybe leave points where the traps ares}

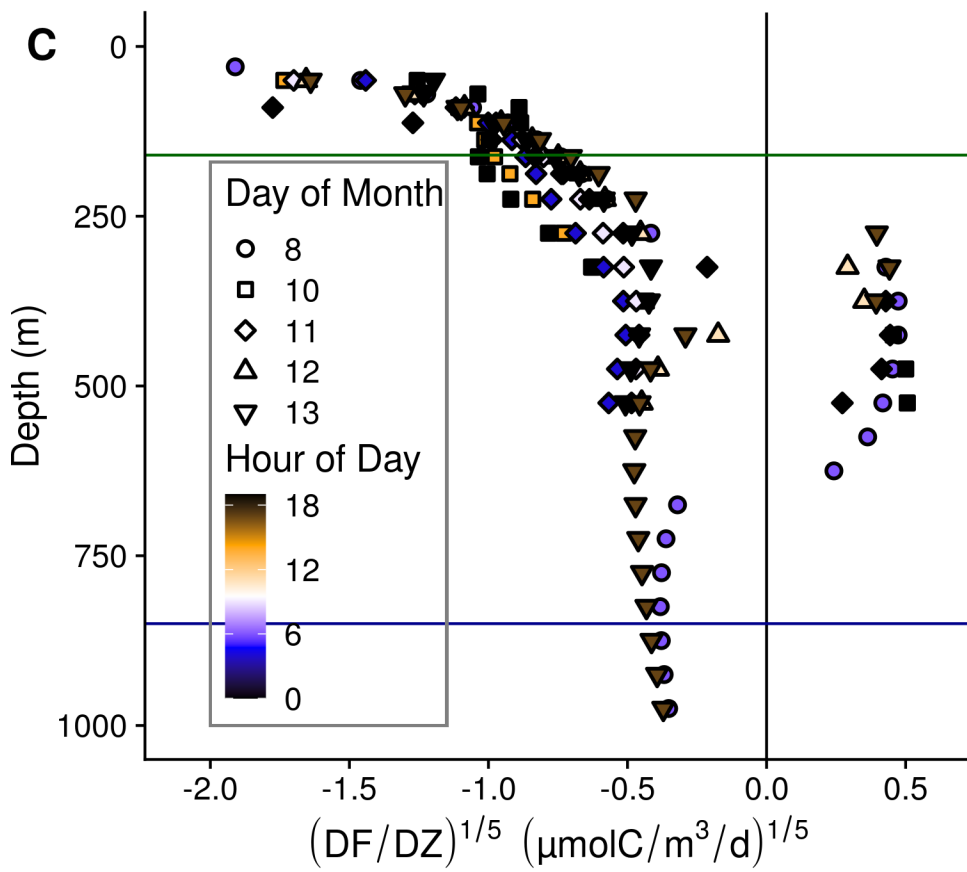
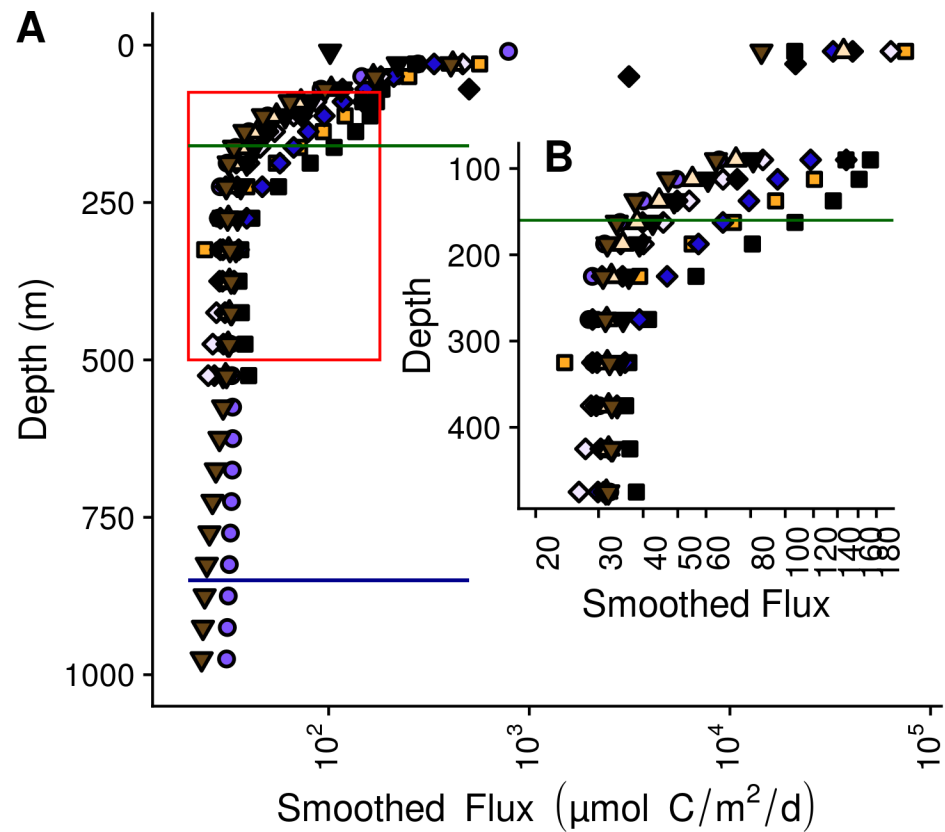


Figure 4. Within and between day variability in UVP predicted particle flux at ETNP station P2. Profiles are compared against P16 station 100, a non OMZ station at similar latitude in the tropical pacific. All profiles are depth binned with higher resolution towards the surface (methods). **(A)** Flux profiles in the top 1000m of the water column. **(B)** A more detailed depiction of the area enclosed by the rectangle in **A**. **(C)** The rate of change of flux, divided by the rate in change in depth. We show the fifth root of these values in order to highlight differences between values close to zero.

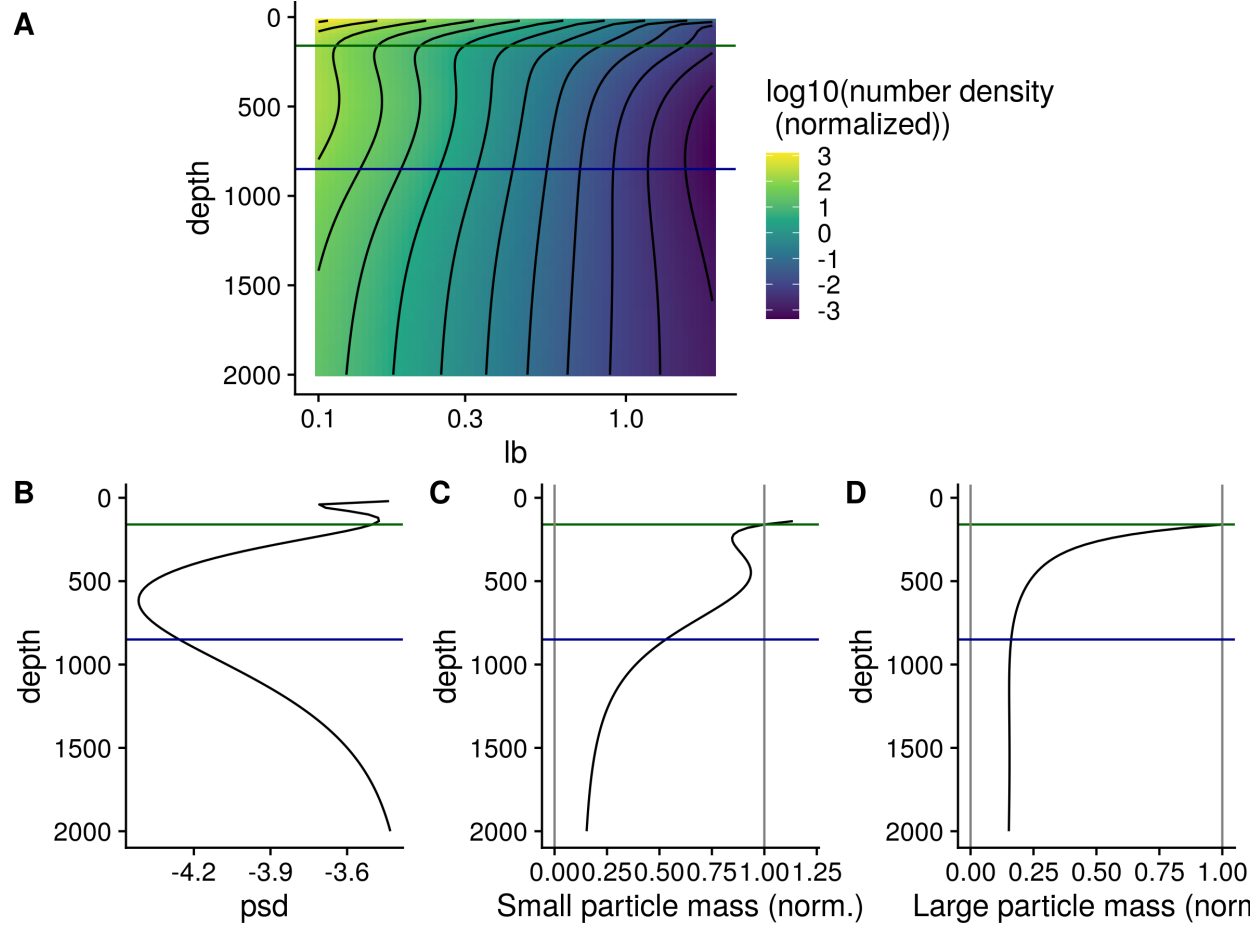


Figure 5. **(A)** GAM smoothed bin-size and volume particle numbers at each particle size class. **(B)** Particle size distributions. And estimated biomass of **(C)** Small and **(D)** Large particles.

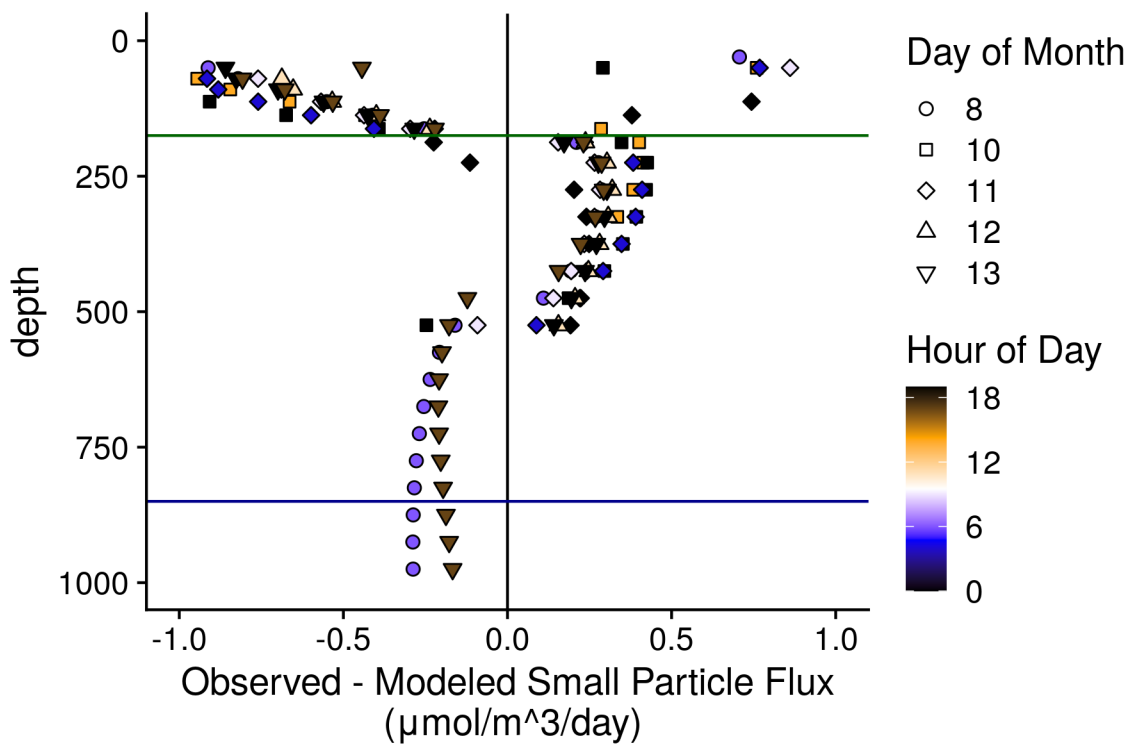


Figure 9. Quantification of non remineralization and sinking like processes. Points indicate the difference between the observed small particle flux, and the flux that would be estimated if particles from the size distribution in the depth bin above remineralized and sank only following the PRISM model. Values are normalized to the change in depth. Thus values are $\mu\text{mol Carbon}/\text{m}^3/\text{day}$ {change to “Deviation from Model”, keep units}

Supplemental Figs

[move to supplement]

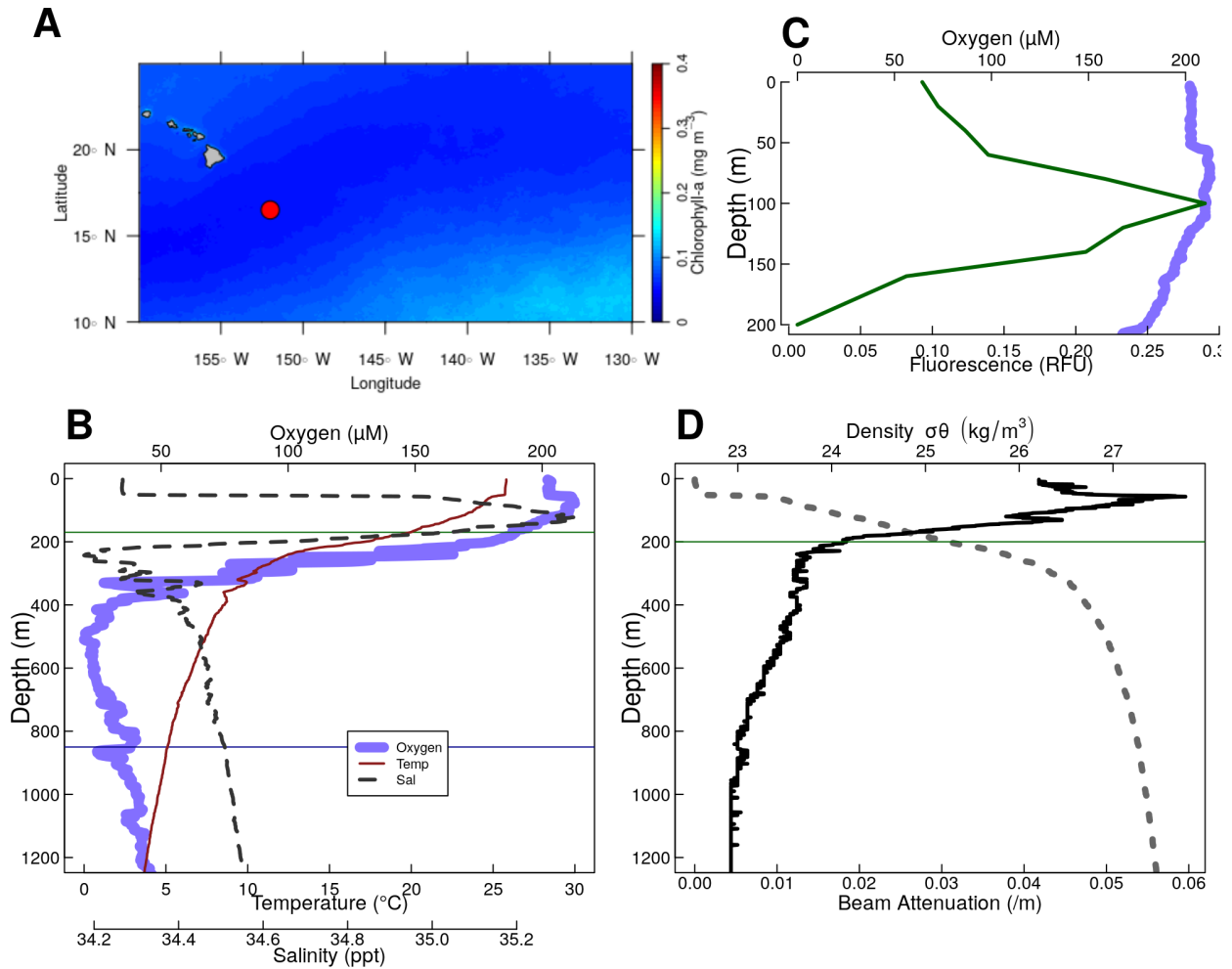


Figure S1. Physical and chemical data from P16 Station 100. Located at 16.5°N 152.0°W. (A) Map of the nearby tropical pacific station P6 Station 100. Colors indicate chlorophyll concentrations at the surface, averaged over all MODIS images. The red circle indicates the location of Station P2. (B-D) Oceanographic parameters. The thin horizontal green line shows the location of the base of the photic zone (200m m). **A** Oxygen, and fluorescence. Because the fluorometer was broken on this cruise, fluorescence data were pulled from world ocean atlas. **B** Oxygen temperature and salinity. **(C)** Beam attenuation and density, calculated from the salinity temperature and pressure data.

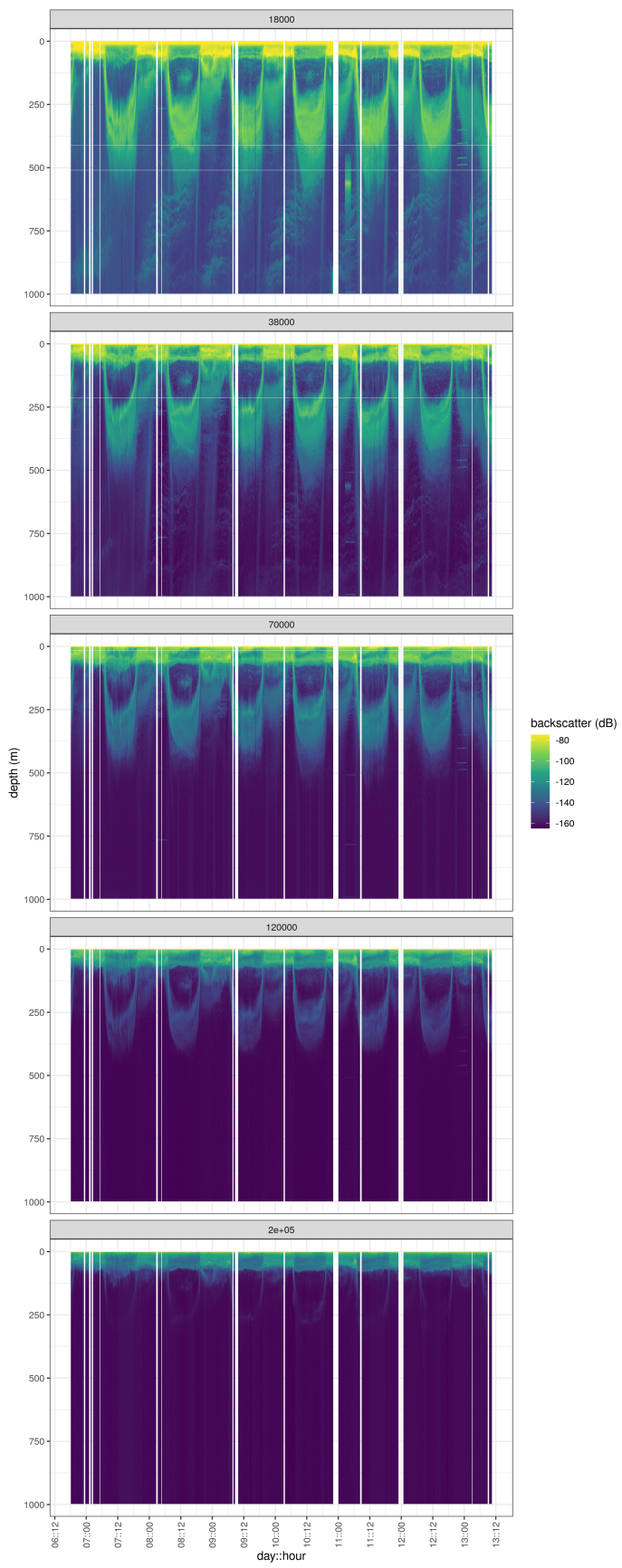


Figure S2. Acoustic data, measured by EK60, measured over the course of the experiment. Shown are data from the all frequency bands. Values are in return signal intensity and have not been normalized to observed biomass.

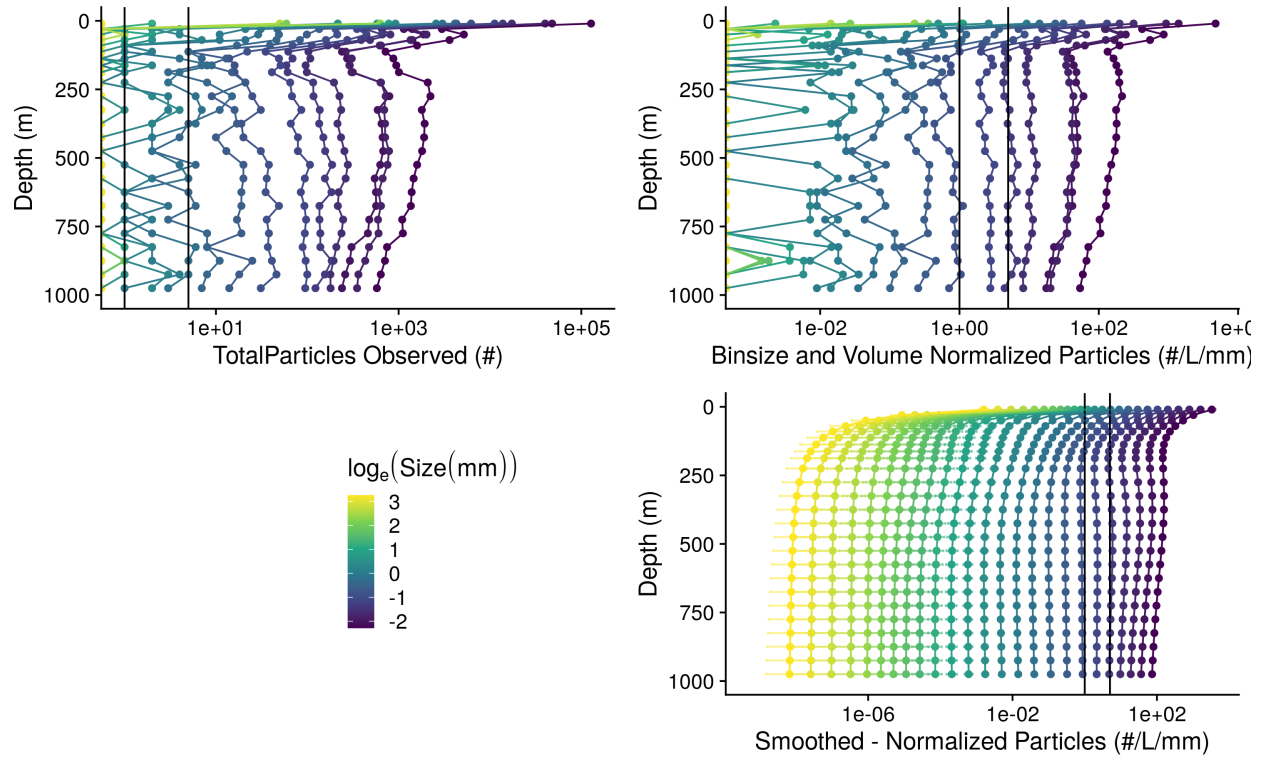


Figure S3. A profile of particle abundances at different sizes and depths. **(A)** Numbers of observed particles and **(B)** particle numbers normalized to volume sampled and particle size bin width. **(C)** Smoothed and extrapolated particle abundances, based on a negative binomial GAM that predicts particle abundance form size and depth.

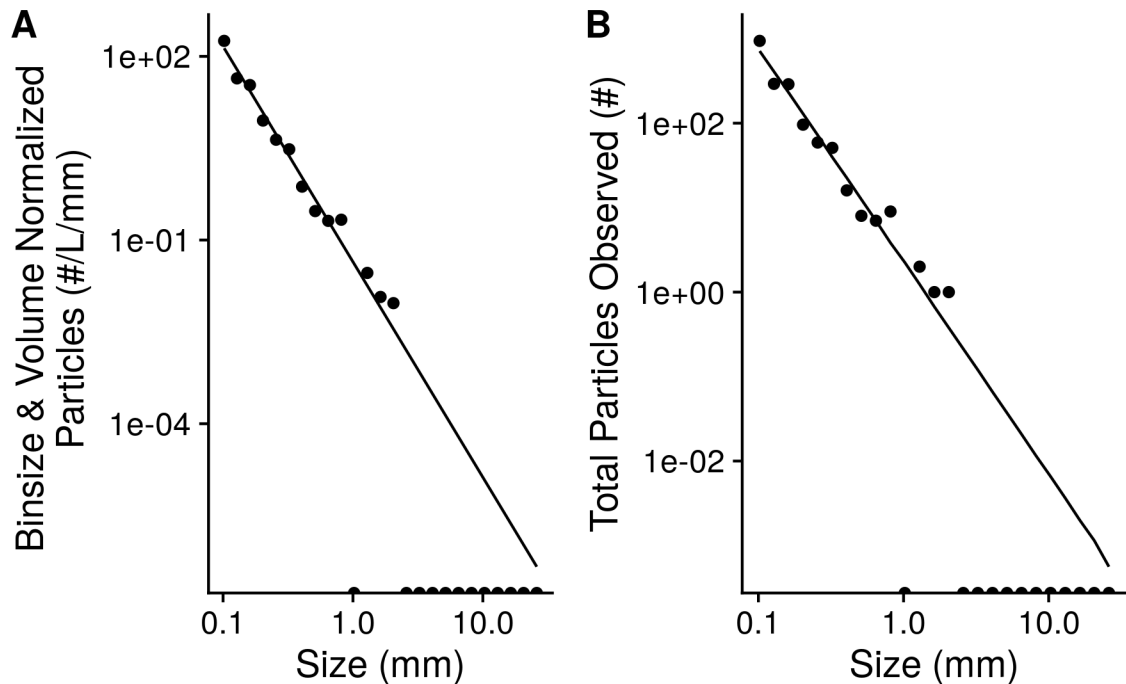


Figure S4. An example of observed particle size distribution spectra. These are depth binned data from between X and X m deep in the water column from the cast that occurred at *DATETIME* for *stn_043*. A total volume of XXX L of water are sampled herein. Points indicate (A) total numbers of observed particles and (B) particle numbers normalized to volume sampled and particle size bin width. The line indicates the predicted best fit line of the data. The line was fit on the bin and volume normalized data by a negative-binomial general linear model. The line in panel A indicates predictions from this same model, re-scaled into absolute particle space.

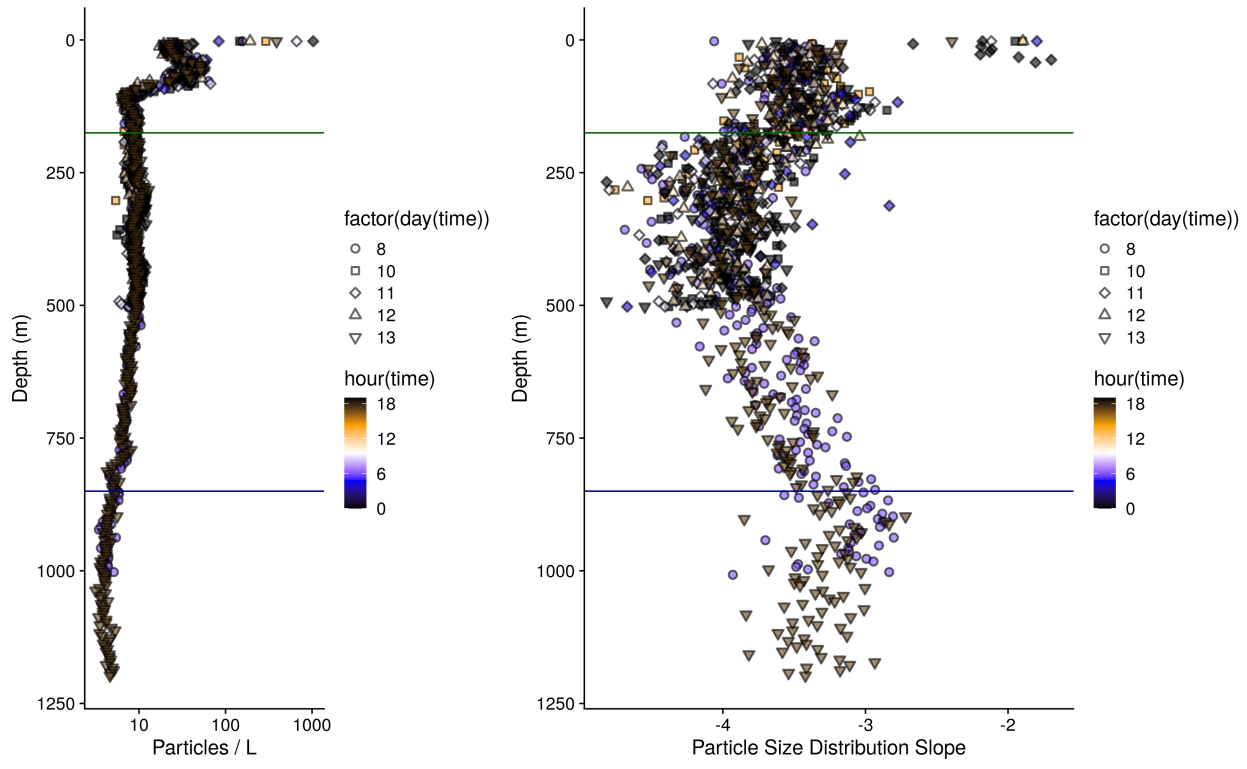


Figure S5. (A) Observed, volume normalized total particle numbers from 9 casts taken at different times of the day at ETNP station P2. (B) Calculated particle size distribution slopes of those particles. These data have not been binned by depth. {Axes are backward}

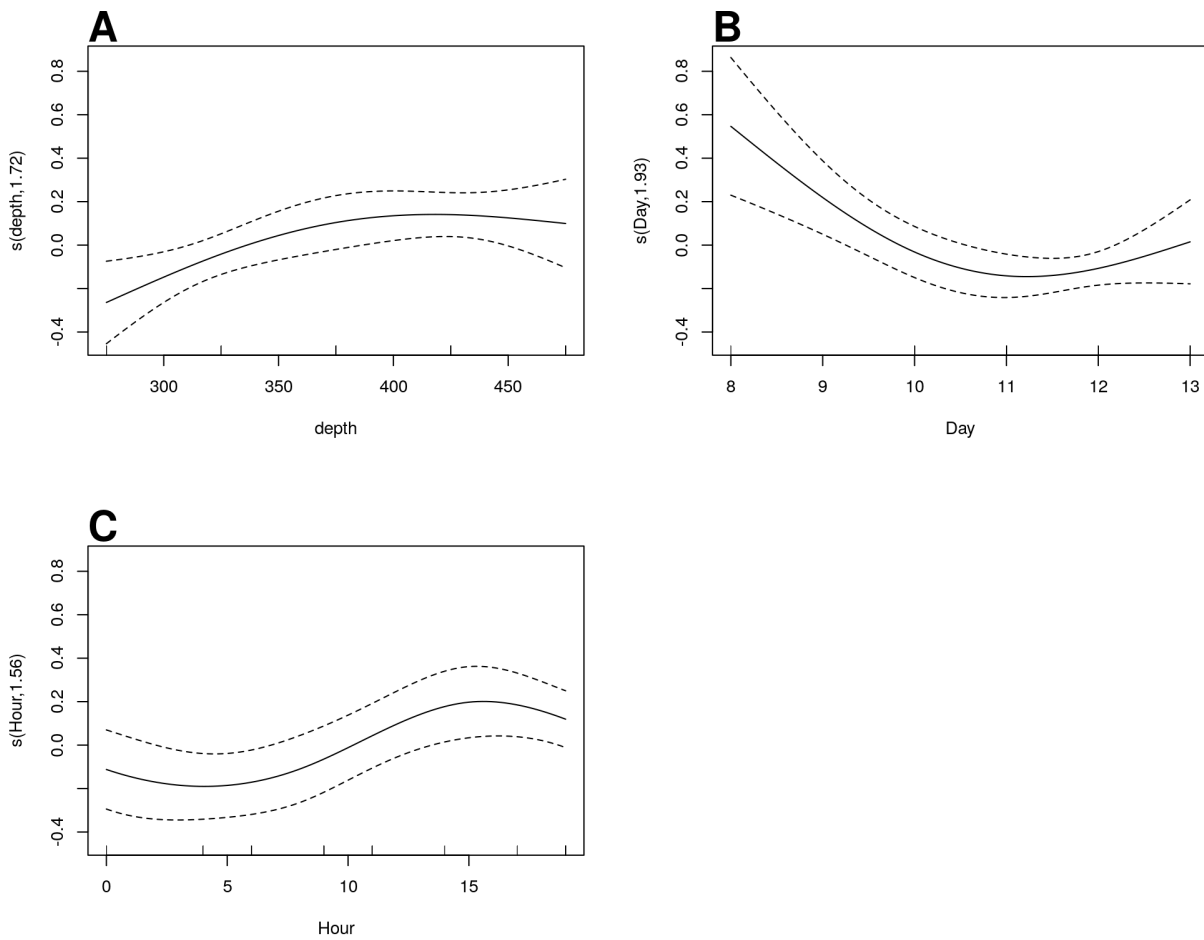


Figure S6. GAM predicted effects of **A** Depth, **B** Day of the month in January 2017, and **C** hour of the day on the fifth-root transformed, depth normalized, rate of change of flux. Y axis indicates the value of the component smooth functions effect on Flux. Positive values associate with times and regions of the water column where flux is increasing, holding other factors constant, and negative ones where it is decreasing.

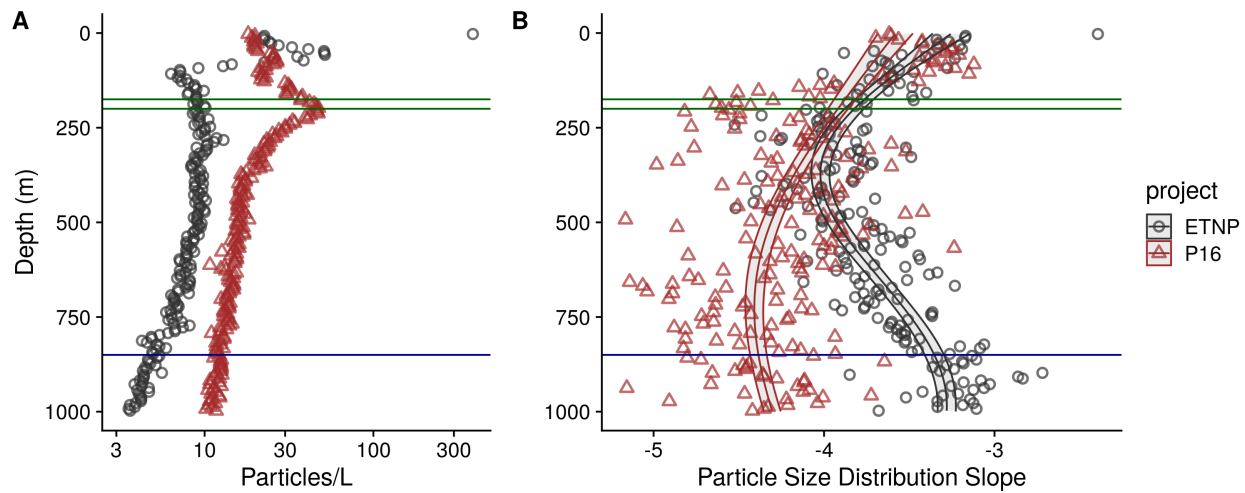


Figure S7. As above, but for the final cast taken at ETNP station P2 and the only cast collected from the

P16 transect at the station 100. P16 Station 100 was chosen because it is at a similar latitude to ETNP station P2. (A) Total particle numbers, (B) Particle size distribution. **{Cut to 1000m}**

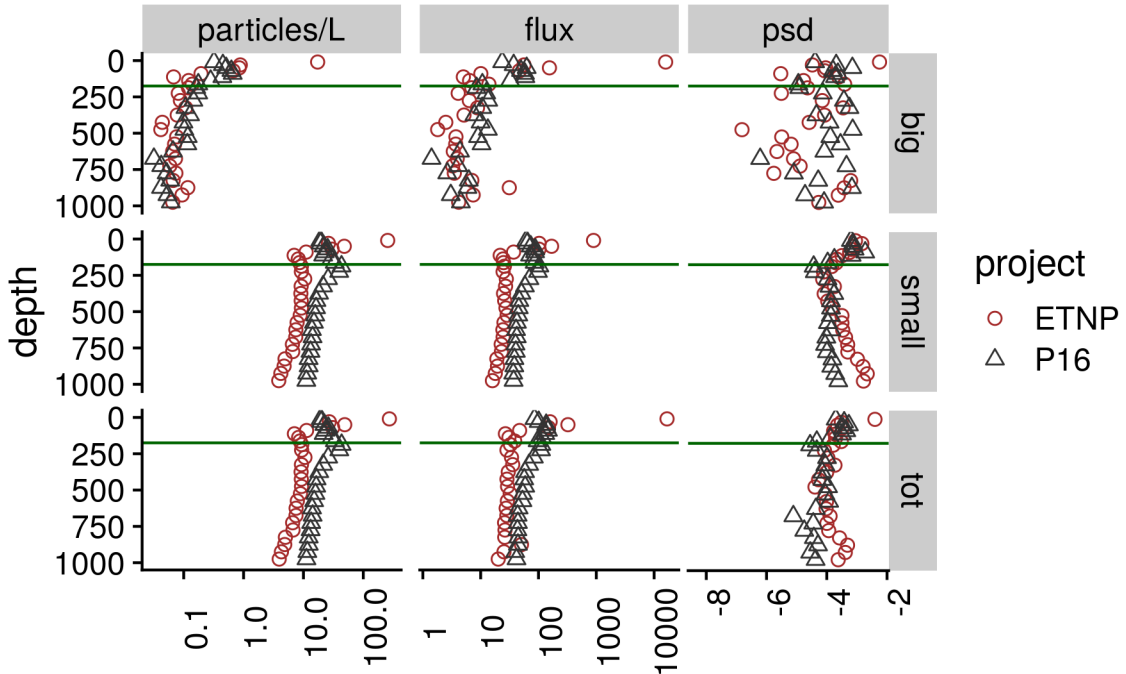


Figure S8. Depth binned particle number (volume normalized), particle size slope (PSD), and flux (estimated as in Fig. 4) for large ($\geq 500 \mu\text{m}$), small ($< 500 \mu\text{m}$) and total particles, at the oxic and anoxic site

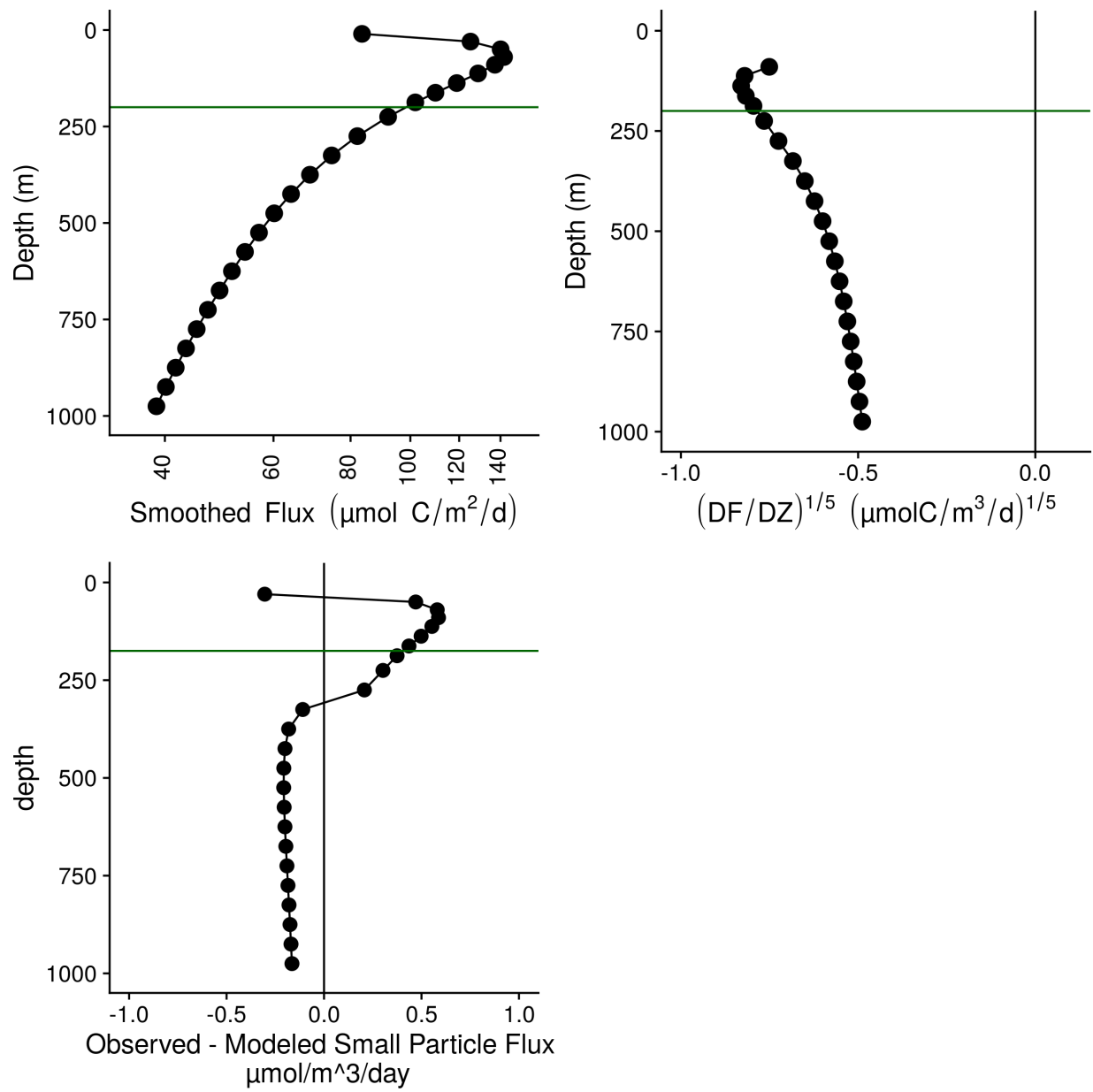


Figure S9. Flux profiles and flux attenuation at P2 Station 100. **(A)** Flux profile **(B)** Fifth-root transformed depth normalized rate of flux decrease. **(C)** Difference between observed and modeled results. Higher values suggest more disaggregation-like processes.

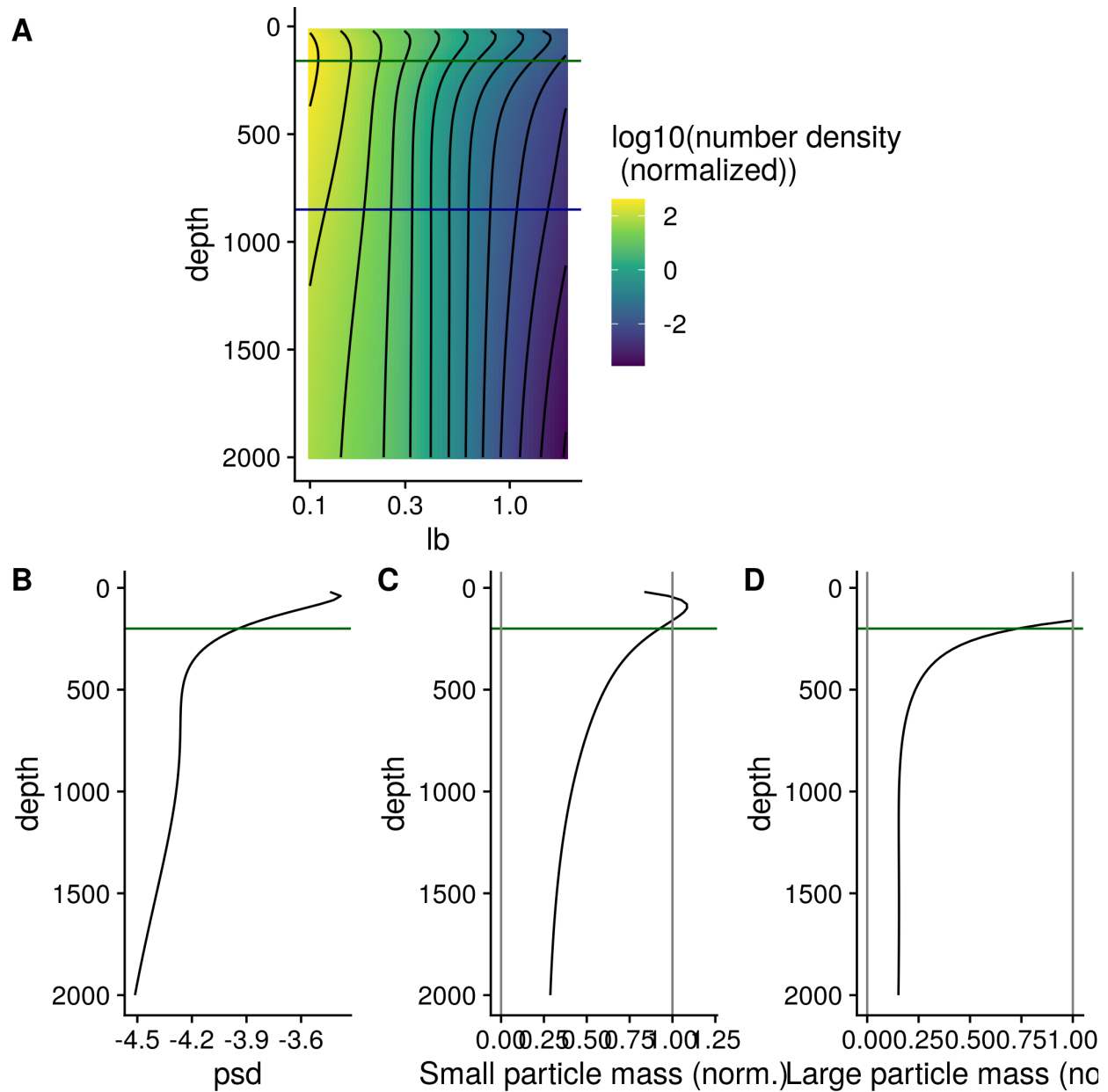


Figure S10. The same profiles as shown in Figure 5, but for the oxic site P16 Station 100. **(A)** GAM smoothed bin-size and volume particle numbers at each particle size class. **(B)** Particle size distributions. And estimated biomass of **(C)** Small and **(D)** Large particles.

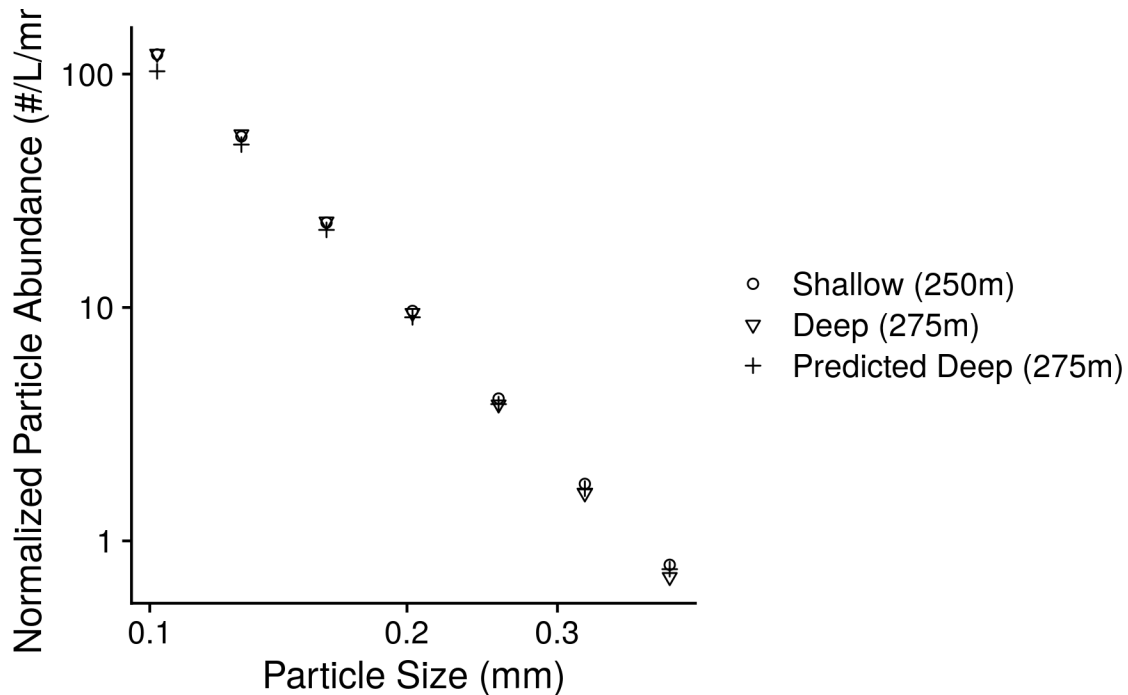


Figure S11. An example of differences between modeled and observed particle slope. Shown are profiles of particles between $100 \mu\text{m}$ and $500 \mu\text{m}$ than 1 mm . The particle size distribution at a shallow and deeper depth are shown. The model generates a prediction of the deep depth profile form the shallow depth profile and the flux attenuation between the two profiles. The model predicts more attenuation of the smallest particles than it actually observed.

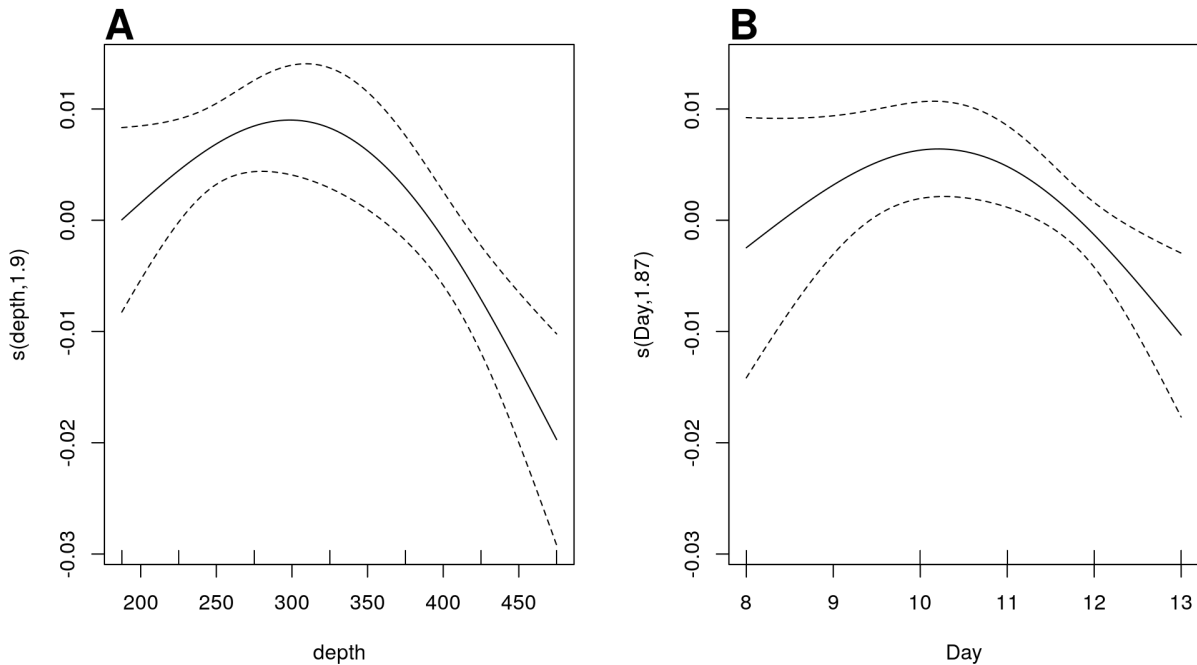


Figure S12. GAM predicted effects of **A** Depth, **B** Day of the month in January 2017 Y axis indicates the

value of the component smooth functions effect on the difference between observed and modeled flux. Thus higher values correspond with greater flux of small particles than predicted by the model.

References

- Antezana, Tarsicio. 2009. "Species-Specific Patterns of Diel Migration into the Oxygen Minimum Zone by Euphausiids in the Humboldt Current Ecosystem." *Progress in Oceanography*, Eastern Boundary Upwelling Ecosystems: Integrative and Comparative Approaches, 83 (1): 228–36. <https://doi.org/10.1016/j.pocean.2009.07.039>.
- Archibald, Kevin M., David A. Siegel, and Scott C. Doney. 2019. "Modeling the Impact of Zooplankton Diel Vertical Migration on the Carbon Export Flux of the Biological Pump." *Global Biogeochemical Cycles* 33 (2): 181–99. <https://doi.org/10.1029/2018GB005983>.
- Bianchi, Daniele, Eric D. Galbraith, David A. Carozza, K. a. S. Mislan, and Charles A. Stock. 2013. "Intensification of Open-Ocean Oxygen Depletion by Vertically Migrating Animals." *Nature Geoscience* 6 (7). Nature Publishing Group: 545–48. <https://doi.org/10.1038/ngeo1837>.
- Bianchi, Daniele, Thomas S. Weber, Rainer Kiko, and Curtis Deutsch. 2018. "Global Niche of Marine Anaerobic Metabolisms Expanded by Particle Microenvironments." *Nature Geoscience* 11 (4). Nature Publishing Group: 263. <https://doi.org/10.1038/s41561-018-0081-0>.
- Burd, Adrian B., and George A. Jackson. 2009. "Particle Aggregation." *Annual Review of Marine Science* 1 (1): 65–90. <https://doi.org/10.1146/annurev.marine.010908.163904>.
- Cavan, Emma L., Stephanie A. Henson, Anna Belcher, and Richard Sanders. 2017. "Role of Zooplankton in Determining the Efficiency of the Biological Carbon Pump." *Biogeosciences* 14 (January): 177–86. <https://doi.org/10.5194/bg-14-177-2017>.
- Cisewski, Boris, Volker H. Strass, Monika Rhein, and Sören Krägesky. 2010. "Seasonal Variation of Diel Vertical Migration of Zooplankton from ADCP Backscatter Time Series Data in the Lazarev Sea, Antarctica." *Deep Sea Research Part I: Oceanographic Research Papers* 57 (1): 78–94. <https://doi.org/10.1016/j.dsr.2009.10.005>.
- Cram, Jacob A., Thomas Weber, Shirley W. Leung, Andrew M. P. McDonnell, Jun-Hong Liang, and Curtis Deutsch. 2018. "The Role of Particle Size, Ballast, Temperature, and Oxygen in the Sinking Flux to the Deep Sea." *Global Biogeochemical Cycles* 32 (5): 858–76. <https://doi.org/10.1029/2017GB005710>.
- DeVries, Timothy, and Thomas Weber. 2017. "The Export and Fate of Organic Matter in the Ocean: New Constraints from Combining Satellite and Oceanographic Tracer Observations." *Global Biogeochemical Cycles*, January, 2016GB005551. <https://doi.org/10.1002/2016GB005551>.
- DeVries, T., J.-H. Liang, and C. Deutsch. 2014. "A Mechanistic Particle Flux Model Applied to the Oceanic Phosphorus Cycle." *Biogeosciences Discuss.* 11 (3): 3653–99. <https://doi.org/10.5194/bgd-11-3653-2014>.
- Dilling, Lisa, and Alice L Alldredge. 2000. "Fragmentation of Marine Snow by Swimming Macrozooplankton: A New Process Impacting Carbon Cycling in the Sea." *Deep Sea Research Part I: Oceanographic Research Papers* 47 (7): 1227–45. [https://doi.org/10.1016/S0967-0637\(99\)00105-3](https://doi.org/10.1016/S0967-0637(99)00105-3).
- Francois, Roger, Susumu Honjo, Richard Krishfield, and Steve Manganini. 2002. "Factors Controlling the Flux of Organic Carbon to the Bathypelagic Zone of the Ocean." *Global Biogeochemical Cycles* 16 (4): 34–31–34–20. <https://doi.org/10.1029/2001GB001722>.
- Fuchsman, Clara A., Hilary I. Palevsky, Brittany Widner, Megan Duffy, Michael C. G. Carlson, Jacquelyn A. Neibauer, Margaret R. Mulholland, Richard G. Keil, Allan H. Devol, and Gabrielle Rocap. 2019. "Cyanobacteria and Cyanophage Contributions to Carbon and Nitrogen Cycling in an Oligotrophic Oxygen-Deficient Zone." *The ISME Journal*, June, 1. <https://doi.org/10.1038/s41396-019-0452-6>.

- Gilly, William F., J. Michael Beman, Steven Y. Litvin, and Bruce H. Robison. 2013. "Oceanographic and Biological Effects of Shoaling of the Oxygen Minimum Zone." *Annual Review of Marine Science* 5 (1): 393–420. <https://doi.org/10.1146/annurev-marine-120710-100849>.
- Goldthwait, S. A., C. A. Carlson, G. K. Henderson, and A. L. Alldredge. 2005. "Effects of Physical Fragmentation on Remineralization of Marine Snow." *Marine Ecology Progress Series* 305. Inter-Research Science Center: 59–65.
- Guidi, Lionel, George A. Jackson, Lars Stemmann, Juan Carlos Miquel, Marc Picheral, and Gabriel Gorsky. 2008. "Relationship Between Particle Size Distribution and Flux in the Mesopelagic Zone." *Deep Sea Research Part I: Oceanographic Research Papers* 55 (10): 1364–74. <https://doi.org/10.1016/j.dsr.2008.05.014>.
- Hannides, Cecelia C.S., Michael R. Landry, Claudia R. Benitez-Nelson, Renée M. Styles, Joseph P. Montoya, and David M. Karl. 2009. "Export Stoichiometry and Migrant-Mediated Flux of Phosphorus in the North Pacific Subtropical Gyre." *Deep Sea Research Part I: Oceanographic Research Papers* 56 (1): 73–88. <https://doi.org/10.1016/j.dsr.2008.08.003>.
- Hartnett, Hilairy Ellen. 1998. "Organic Carbon Input, Degradation, and Preservation in Continental Margin Sediments: An Assessment of the Role of a Strong Oxygen Deficient Zone." Thesis.
- Hays, Graeme C. 2003. "A Review of the Adaptive Significance and Ecosystem Consequences of Zooplankton Diel Vertical Migrations." In *Migrations and Dispersal of Marine Organisms*, edited by M. B. Jones, A. Ingólfsson, E. Ólafsson, G. V. Helgason, K. Gunnarsson, and J. Svavarsson, 163–70. Developments in Hydrobiology. Dordrecht: Springer Netherlands. https://doi.org/10.1007/978-94-017-2276-6_18.
- Herrera, Inma, Lidia Yebra, Tarsicio Antezana, Alan Giraldo, Jaime Färber-Lorda, and Santiago Hernández-León. 2019. "Vertical Variability of Euphausia Distinguenda Metabolic Rates During Diel Migration into the Oxygen Minimum Zone of the Eastern Tropical Pacific Off Mexico." *Journal of Plankton Research* 41 (2): 165–76. <https://doi.org/10.1093/plankt/fbz004>.
- Heywood, Karen J. 1996. "Diel Vertical Migration of Zooplankton in the Northeast Atlantic." *Journal of Plankton Research* 18 (2): 163–84. <https://doi.org/10.1093/plankt/18.2.163>.
- Hidalgo, Pamela, Ruben Escribano, and Carmen E. Morales. 2005. "Ontogenetic Vertical Distribution and Diel Migration of the Copepod Eucalanus Inermis in the Oxygen Minimum Zone Off Northern Chile (2021)." *Journal of Plankton Research* 27 (6): 519–29. <https://doi.org/10.1093/plankt/fbi025>.
- Inthorn, Maik. 2005. "Lateral Particle Transport in Nepheloid Layers - a Key Factor for Organic Matter Distribution and Quality in the Benguela High-Productivity Area." October. Universität Bremen.
- Jackson, George A., and Adrian B. Burd. 2001. "A Model for the Distribution of Particle Flux in the Mid-Water Column Controlled by Subsurface Biotic Interactions." *Deep Sea Research Part II: Topical Studies in Oceanography*, The US JGOFS Synthesis and Modeling Project: Phase 1, 49 (1): 193–217. [https://doi.org/10.1016/S0967-0645\(01\)00100-X](https://doi.org/10.1016/S0967-0645(01)00100-X).
- Jiang, Songnian, Tommy D. Dickey, Deborah K. Steinberg, and Laurence P. Madin. 2007. "Temporal Variability of Zooplankton Biomass from ADCP Backscatter Time Series Data at the Bermuda Testbed Mooring Site." *Deep Sea Research Part I: Oceanographic Research Papers* 54 (4): 608–36. <https://doi.org/10.1016/j.dsr.2006.12.011>.
- Kaartvedt, Stein, Thor A. Klevjer, Thomas Torgersen, Tom A. Sørnes, and Anders Røstad. 2007. "Diel Vertical Migration of Individual Jellyfish (*Periphylla Periphylla*)."*Limnology and Oceanography* 52 (3): 975–83. <https://doi.org/10.4319/lo.2007.52.3.0975>.
- Keil, Richard G., Jacquelyn A. Neibauer, and Allan H. Devol. 2016. "A Multiproxy Approach to Understanding the "Enhanced" Flux of Organic Matter Through the Oxygen-Deficient Waters of the Arabian Sea." *Biogeosciences* 13 (7): 2077–92. <https://doi.org/http://dx.doi.org/10.5194/bg-13-2077-2016>.
- Kiko, Rainer, Peter Brandt, Svenja Christiansen, Jannik Faustmann, Iris Kriest, Elizandro Rodrigues, Florian Schütte, and Helena Hauss. 2020. "Zooplankton-Mediated Fluxes in the Eastern Tropical North Atlantic." *Frontiers in Marine Science* 7 (May). <https://doi.org/10.3389/fmars.2020.00358>.

- Kiko, R., A. Biastoch, P. Brandt, S. Cravatte, H. Hauss, R. Hummels, I. Kriest, et al. 2017. "Biological and Physical Influences on Marine Snowfall at the Equator." *Nature Geoscience* 10 (11): 852–58. <https://doi.org/10.1038/ngeo3042>.
- Kwon, Eun Young, François Primeau, and Jorge L. Sarmiento. 2009. "The Impact of Remineralization Depth on the AirSea Carbon Balance." *Nature Geoscience* 2 (9): 630–35. <https://doi.org/10.1038/ngeo612>.
- Maas, Amy E., Sarah L. Frazar, Dawn M. Outram, Brad A. Seibel, and Karen F. Wishner. 2014. "Fine-Scale Vertical Distribution of Macroplankton and Microneuston in the Eastern Tropical North Pacific in Association with an Oxygen Minimum Zone." *Journal of Plankton Research* 36 (6): 1557–75. <https://doi.org/10.1093/plankt/fbu077>.
- McDonnell, Andrew M. P., and Ken O. Buesseler. 2010. "Variability in the Average Sinking Velocity of Marine Particles." *Limnology and Oceanography* 55 (5): 2085–96. <https://doi.org/10.4319/lo.2010.55.5.2085>.
- Neuer, Susanne, Morten Iversen, and Gerhard Fischer. 2014. "The Ocean's Biological Carbon Pump as Part of the Global Carbon Cycle." *Limnology and Oceanography E-Lectures* 4 (4): 1–51. <https://doi.org/10.4319/lol.2014.sneuer.miversen.gfischer.9>.
- Passow, Uta, and Ca Carlson. 2012. "The Biological Pump in a High CO₂ World." *Marine Ecology Progress Series* 470 (December): 249–71. <https://doi.org/10.3354/meps09985>.
- Pennington, J. Timothy, Kevin L. Mahoney, Victor S. Kuwahara, Dorota D. Kolber, Ruth Calienes, and Francisco P. Chavez. 2006. "Primary Production in the Eastern Tropical Pacific: A Review." *Progress in Oceanography* 69 (2-4): 285–317. <https://doi.org/10.1016/j.pocean.2006.03.012>.
- Picheral, Marc, Lionel Guidi, Lars Stemmann, David M. Karl, Ghislaine Iddaoud, and Gabriel Gorsky. 2010. "The Underwater Vision Profiler 5: An Advanced Instrument for High Spatial Resolution Studies of Particle Size Spectra and Zooplankton." *Limnology and Oceanography: Methods* 8 (9): 462–73. <https://doi.org/10.4319/lom.2010.8.462>.
- Picheral, M., S Colin, and J-O Irisson. n.d. "EcoTaxa, a Tool for the Taxonomic Classification of Images."
- Rabindranath, Ananda, Malin Daase, Stig Falk-Petersen, Anette Wold, Margaret I. Wallace, Jørgen Berge, and Andrew S. Brierley. 2011. "Seasonal and Diel Vertical Migration of Zooplankton in the High Arctic During the Autumn Midnight Sun of 2008." *Marine Biodiversity* 41 (3): 365–82. <https://doi.org/10.1007/s12526-010-0067-7>.
- Riquelme-Bugueño, Ramiro, Iván Pérez-Santos, Nicolás Alegría, Cristian A. Vargas, Mauricio A. Urbina, and Rubén Escribano. 2020. "Diel Vertical Migration into Anoxic and High- P CO₂ Waters: Acoustic and Net-Based Krill Observations in the Humboldt Current." *Scientific Reports* 10 (1). Nature Publishing Group: 17181. <https://doi.org/10.1038/s41598-020-73702-z>.
- Sainmont, Julie, Astthor Gislason, Jan Heuschele, Clare N. Webster, Peter Sylvander, Miao Wang, and Øystein Varpe. 2014. "Inter- and Intra-Specific Diurnal Habitat Selection of Zooplankton During the Spring Bloom Observed by Video Plankton Recorder." *Marine Biology* 161 (8): 1931–41. <https://doi.org/10.1007/s00227-014-2475-x>.
- Siegel, D. A., Ken O. Buesseler, Michael J. Behrenfeld, Claudia R. Benitez-Nelson, Emmanuel Boss, Mark A. Brzezinski, Adrian Burd, et al. 2016. "Prediction of the Export and Fate of Global Ocean Net Primary Production: The EXPORTS Science Plan." *Frontiers in Marine Science* 3. <https://doi.org/10.3389/fmars.2016.00022>.
- Steinberg, Deborah K., Craig A. Carlson, Nicholas R. Bates, Sarah A. Goldthwait, Laurence P. Madin, and Anthony F. Michaels. 2000. "Zooplankton Vertical Migration and the Active Transport of Dissolved Organic and Inorganic Carbon in the Sargasso Sea." *Deep Sea Research Part I: Oceanographic Research Papers* 47 (1): 137–58. [https://doi.org/10.1016/S0967-0637\(99\)00052-7](https://doi.org/10.1016/S0967-0637(99)00052-7).
- Steinberg, Deborah K., and Michael R. Landry. 2017. "Zooplankton and the Ocean Carbon Cycle." *Annual Review of Marine Science* 9: 413–44. <https://doi.org/10.1146/annurev-marine-010814-015924>.

- Steinberg, Deborah K., Benjamin A. S. Van Mooy, Ken O. Buesseler, Philip W. Boyd, Toru Kobari, and David M. Karl. 2008. "Bacterial Vs. Zooplankton Control of Sinking Particle Flux in the Ocean's Twilight Zone." *Limnology and Oceanography* 53 (4): 1327–38. <https://doi.org/10.2307/40058255>.
- Stramma, Lothar, Gregory C. Johnson, Janet Sprintall, and Volker Mohrholz. 2008. "Expanding Oxygen-Minimum Zones in the Tropical Oceans." *Science* 320 (5876): 655–58. <https://doi.org/10.1126/science.1153847>.
- Stukel, Michael R., Moira Décima, Michael R. Landry, and Karen E. Selph. 2018. "Nitrogen and Isotope Flows Through the Costa Rica Dome Upwelling Ecosystem: The Crucial Mesozooplankton Role in Export Flux." *Global Biogeochemical Cycles* 32 (12): 1815–32. <https://doi.org/10.1029/2018GB005968>.
- Stukel, Michael R., Mark D. Ohman, Thomas B. Kelly, and Tristan Biard. 2019. "The Roles of Suspension-Feeding and Flux-Feeding Zooplankton as Gatekeepers of Particle Flux into the Mesopelagic Ocean in the Northeast Pacific." *Frontiers in Marine Science* 6. Frontiers. <https://doi.org/10.3389/fmars.2019.00397>.
- Turner, Jefferson T. 2015. "Zooplankton Fecal Pellets, Marine Snow, Phytodetritus and the Ocean's Biological Pump." *Progress in Oceanography* 130 (January): 205–48. <https://doi.org/10.1016/j.pocean.2014.08.005>.
- Van Mooy, Benjamin A. S., Richard G Keil, and Allan H Devol. 2002. "Impact of Suboxia on Sinking Particulate Organic Carbon: Enhanced Carbon Flux and Preferential Degradation of Amino Acids via Denitrification." *Geochimica et Cosmochimica Acta* 66 (3): 457–65. [https://doi.org/10.1016/S0016-7037\(01\)00787-6](https://doi.org/10.1016/S0016-7037(01)00787-6).
- Weber, Thomas, and Daniele Bianchi. 2020. "Efficient Particle Transfer to Depth in Oxygen Minimum Zones of the Pacific and Indian Oceans." *Frontiers in Earth Science* 8. Frontiers. <https://doi.org/10.3389/feart.2020.00376>.
- Wilson, Stephanie E., Deborah K. Steinberg, and Ken O. Buesseler. 2008. "Changes in Fecal Pellet Characteristics with Depth as Indicators of Zooplankton Repackaging of Particles in the Mesopelagic Zone of the Subtropical and Subarctic North Pacific Ocean." *Deep Sea Research Part II: Topical Studies in Oceanography* 55 (14-15): 1636–47. <https://doi.org/10.1016/j.dsr2.2008.04.019>.
- Wishner, Karen F., Dawn M. Outram, Brad A. Seibel, Kendra L. Daly, and Rebecca L. Williams. 2013. "Zooplankton in the Eastern Tropical North Pacific: Boundary Effects of Oxygen Minimum Zone Expansion." *Deep Sea Research Part I: Oceanographic Research Papers* 79 (September): 122–40. <https://doi.org/10.1016/j.dsr.2013.05.012>.
- Yang, Chenghao, Dongfeng Xu, Zuozhi Chen, Jun Wang, Mingquan Xu, Yaochu Yuan, and Meng Zhou. 2019. "Diel Vertical Migration of Zooplankton and Micronekton on the Northern Slope of the South China Sea Observed by a Moored ADCP." *Deep Sea Research Part II: Topical Studies in Oceanography* 167 (September): 93–104. <https://doi.org/10.1016/j.dsr2.2019.04.012>.